Noname manuscript No.
(will be inserted by the editor)

A catalogue of nonseparable positive semidefinite kernels on the product of two spheres

Xavier Emery · Ana Paula Peron · Emilio Porcu

Received: date / Accepted: date

Abstract We present a catalogue of 26 parametric families of matrix-valued positive semidefinite kernels for modeling the spatial correlation structure of vector random fields defined over the product of two hyperspheres. Such a geometry has been proved successful to account for complex sources of seasonality and direction-dependence of phenomena regionalized on a large portion of planet Earth. All the kernels are nonseparable, as they cannot be written as the product of positive semidefinite kernels defined on hyperspheres, and sufficient validity conditions on their parameters are identified. Their analytical spectral representations and a spectral simulation algorithm are also provided. A side product is the derivation of new matrix-valued isotropic covariance kernels on hyperspheres, together with their analytical spectral representations.

Keywords Space-time random fields · Matrix-valued covariance kernels · Schoenberg sequences · Spectral simulation · Hypertorus

Mathematics Subject Classification (2010) 60G60 · 62H11 · 86A32

Xavier Emery
Department of Mining Engineering, University of Chile, Avenida Beauchef 850, Santiago, Chile.
Advanced Mining Technology Center, University of Chile, Avenida Beauchef 850, Santiago, Chile.
Tel.: +56-229784498
E-mail: xemery@ing.uchile.cl

Ana Paula Peron
Department of Mathematics, Institute of Mathematical and Computer Sciences, University of São Paulo, Brazil.
E-mail: apperon@icmc.usp.br.

Emilio Porcu
Department of Mathematics, Khalifa University, Abu Dhabi, United Arab Emirates.
E-mail: emilio.porcu@ku.ac.ae

1 Introduction: scope, state-of-the-art, outline

Positive semidefinite kernels are of broad interest in several fields of mathematics, such as operator theory (Aronszajn, 1950), approximation theory (Erb and Filbir, 2008), coding theory (Musin, 2008a) and distance geometry (Musin, 2008b), as well as in computer experiments (Haaland and Qian, 2011), machine learning (Hofmann et al., 2008), spatial and space-time statistics (Chen et al., 2021; Porcu et al., 2021), the latter field being the primary motivation of this work.

Space-time data in meteorological, hydrological and climate studies often exhibit complex seasonal patterns. A usual approach to account for these patterns is to decompose the variable under study into a periodic deterministic trend and a random residual. Removing the trend (detrending) therefore allows studying the residual with the usual tools and methods of spatial statistics. Another approach advocated by Porcu and White (2022) is to embed spatial or space-time domains into a circle or a product of circles, i.e., to trade the traditional Euclidean geometry of the time coordinates for a periodic geometry.

The idea of embedding time periodicities inside the geometry of the space where the data are collected is not novel. In particular, Shirota and Gelfand (2017) have applied such a methodology to model daily crime events using log-Gaussian Cox processes. Continuous-time monitoring of ground-level ozone concentrations has instead been proposed by White and Porcu (2019).

Other relevant applications in environmental, atmospheric, oceanographic, physical and earth sciences where one would benefit from using random fields indexed with circular or spherical coordinates include the analysis of observations collected over a large portion of the Earth (represented as a two-dimensional sphere), as well as of observations that are direction-dependent (e.g., electromagnetic radiation, temperature gradient, gravity gradient, topographic slope, tectonic plate motion, average wind speed or average ocean current velocity measured in a particular direction represented by a point on a circle or on a sphere). Accordingly, analyzing direction-dependent or seasonal-dependent observations that, at the same time, are scattered over the Earth would result in working with a random field with an index set consisting of the product of the unit circle $\mathbb{S}^1$ with the unit two-dimensional sphere $\mathbb{S}^2$ (sometimes the product of two spheres $\mathbb{S}^2 \times \mathbb{S}^2$) representing TIME×SPACE or DIRECTION×SPACE (Mastrantonio et al., 2016).

An essential challenge for this approach to be successful is to identify the structure of such a random field, in particular, its covariance kernel. One avenue is to define a separable covariance kernel, as the product of a kernel on $\mathbb{S}^1$ and another one on $\mathbb{S}^2$. However, separable kernels are often simplistic and do not allow characterizing complex interactions between the spatial variations on $\mathbb{S}^1$ and that on $\mathbb{S}^2$, hence the interest in finding nonseparable (and not too parameter-intensive) kernels.

To date, simpler geometries than the product of a circle and a sphere have been considered to build up nonseparable covariance kernels. For instance, Shirota and Gelfand (2017) consider random fields defined over $\mathbb{S}^1 \times \mathbb{R}^2$, where

$\mathbb{S}^1$ is time wrapped over the circle and $\mathbb{R}^2$ is the spatial domain (a planar surface). In the same line, Mastrantonio et al. (2019) and White and Porcu (2019) consider a Bayesian hierarchical modeling where seasonality is modeled through conditioning sets. Peron et al. (2018) propose product-sum covariance kernels on $\mathbb{S}^k \times \mathbb{R}$, while Shirota and Gelfand (2017), Porcu et al. (2016), Alegría et al. (2019) and Emery et al. (2021) introduce nonseparable covariance kernels on $\mathbb{S}^k \times \mathbb{R}^\ell$, with k and ℓ two positive integers, motivated by applications that range from climatology to geological engineering.

Yet, random fields defined over $\mathbb{S}^k \times \mathbb{S}^\ell$ have been considered to a limited extent only. Characterizations of the covariance kernels associated with scalar-valued random fields that are continuously indexed over $\mathbb{S}^k \times \mathbb{S}^\ell$ have been provided by Guella et al. (2015) and Guella and Menegatto (2016), while the work by Porcu and White (2022) provides parametric families of such kernels. The contribution by Bachoc et al. (2021) gives spectral representations for vector random fields, together with some specific parametric families of matrix-valued covariance kernels on $\mathbb{S}^k \times \mathbb{S}^\ell$.

This paper provides a catalogue of parametric families of matrix-valued nonseparable covariance kernels associated with vector random fields that are continuously indexed over the product of two (hyper)spheres. The outline is the following. Section 2 contains a succinct mathematical and statistical background. Section 3 lists 26 new families of covariance kernels, together with their spectral representations and sufficient validity conditions. A discussion on these kernels (Section 4), methodological proposals for parameter estimation and for random field simulation (Section 5) and concluding remarks (Section 6) follow. Proofs are deferred to the Appendix to ease legibility.

2 Background

2.1 Positive semidefinite and conditionally negative semidefinite matrices

Throughout, p is a positive integer and bold letters indicate real-valued p-dimensional vectors or symmetric $p \times p$ matrices. All matrix operations (product, ratio, or any function) are taken elementwise. For a $p \times p$ matrix $\boldsymbol{a}$ and a real value ω, $\omega \pm \boldsymbol{a}$ is taken as a shortcut of $\omega\,\mathbf{1} \pm \boldsymbol{a}$, where $\mathbf{1}$ is the all-ones matrix of size $p \times p$.

Let $\boldsymbol{a} = [a_{i,j}]_{i,j=1}^p$ be a symmetric $p \times p$ real matrix, $\boldsymbol{\omega} = [\omega_1, \dots, \omega_p]^\top \in \mathbb{R}^p$ (with $\top$ denoting the transpose operator) and the quadratic form

$$Q(\boldsymbol{a}, \boldsymbol{\omega}) := \sum_{i=1}^p \sum_{j=1}^p \omega_i\, a_{i,j}\, \omega_j. \tag{1}$$

The matrix $\boldsymbol{a}$ is positive semidefinite when $Q(\boldsymbol{a}, \boldsymbol{\omega}) \geq 0$ for any $\boldsymbol{\omega}$. If $Q(\boldsymbol{a}, \boldsymbol{\omega}) > 0$ for any nonzero $\boldsymbol{\omega}$, then the matrix is said to be positive definite. The matrix $\boldsymbol{a}$ is conditionally negative semidefinite when $Q(\boldsymbol{a}, \boldsymbol{\omega}) \leq 0$ for any $\boldsymbol{\omega}$ whose components add to zero. Likewise, $\boldsymbol{a}$ is said to be conditionally negative definite if $Q(\boldsymbol{a},\boldsymbol{\omega}) < 0$ for any nonzero $\boldsymbol{\omega}$ whose components add to zero. The following criteria are useful to establish the positive or conditional negative semidefiniteness of a matrix:

(1) $\boldsymbol{a}$ is conditionally negative (semi)definite if, and only if, $[a_{ip} + a_{pj} - a_{ij} - a_{pp}]_{i,j=1}^{p-1}$ is positive (semi)definite (Reams, 1999, Lemma 2.4);
(2) $\boldsymbol{a}$ is conditionally negative semidefinite if, and only if, $\exp(-t\boldsymbol{a})$ is positive semidefinite for any $t \geq 0$ (Reams, 1999, Lemma 2.5);
(3) $\boldsymbol{a}$ is conditionally negative semidefinite if it has nonnegative entries and $\boldsymbol{a}^2$ is conditionally negative semidefinite (Berg et al., 1984, Chapter 3, Corollary 2.10);
(4) $\boldsymbol{a}$ is conditionally negative (semi)definite if $-\boldsymbol{a}$ is positive (semi)definite;
(5) If $\boldsymbol{a}_1$ and $\boldsymbol{a}_2$ are positive semidefinite, so are $\boldsymbol{a}_1\,\boldsymbol{a}_2$ (Schur product theorem) and $\boldsymbol{a}_1 + \boldsymbol{a}_2$;
(6) If $\boldsymbol{a}_1$ and $\boldsymbol{a}_2$ are conditionally negative semidefinite, so is $\boldsymbol{a}_1 + \boldsymbol{a}_2$;
(7) If $\boldsymbol{a}_1$ and $-\boldsymbol{a}_2$ are positive semidefinite, then $\boldsymbol{a}_1\,\boldsymbol{a}_2$ is conditionally negative semidefinite.

2.2 Positive semidefinite kernels on hypertori

Let k,ℓ be positive integers. We define the (k,ℓ)-hyperspherical torus or (k,ℓ)-hypertorus through the identity

$$\mathbb{T}^{k,\ell} := \mathbb{S}^k \times \mathbb{S}^\ell = \{\mathbf{x} = (x,y) \ : (x,y) \in \mathbb{R}^{k+1} \times \mathbb{R}^{\ell+1},\ \|x\|_{k+1} = \|y\|_{\ell+1} = 1\},$$

where $\|\cdot\|_{k+1}$ and $\|\cdot\|_{\ell+1}$ are the Euclidean norms on $\mathbb{R}^{k+1}$ and $\mathbb{R}^{\ell+1}$ respectively. Here, $\mathbb{S}^k$ and $\mathbb{S}^\ell$ denote the k- and ℓ-dimensional unit spheres embedded in $\mathbb{R}^{k+1}$ and $\mathbb{R}^{\ell+1}$, respectively. The name *hyperspherical torus* is due to the fact that $\mathbb{T}^{1,1}$, the product of two circles, is isomorphic to the classical circular torus.

We identify $\mathbb{R}^{p\times p}$ with the set of all $p \times p$ matrices with real entries and consider a matrix-valued kernel $\boldsymbol{K} : \mathbb{T}^{k,\ell} \times \mathbb{T}^{k,\ell} \to \mathbb{R}^{p\times p}$, defined as

$$\boldsymbol{K}\left(\mathbf{x},\mathbf{x}'\right) = \left[K_{ij}\left(\mathbf{x},\mathbf{x}'\right)\right]_{i,j=1}^{p}, \qquad \mathbf{x},\mathbf{x}' \in \mathbb{T}^{k,\ell}.$$

$\boldsymbol{K}$ is positive semidefinite if, and only if, the matrix $[[K_{ij}\left(\mathbf{x}_m,\mathbf{x}_n\right)]_{i,j=1}^{p}]_{m,n=1}^{N}$ is positive semidefinite for any set of points $\mathbf{x}_1,\ldots,\mathbf{x}_N \in \mathbb{T}^{k,\ell}$. The Kolmogorov extension theorem states that such a positive semidefinite kernel is the covariance of a Gaussian vector random field $\boldsymbol{Z} = [Z_1,\ldots,Z_p]^\top$ on $\mathbb{T}^{k,\ell}$, i.e.

$$K_{ij}\left(\mathbf{x},\mathbf{x}'\right) = \mathbb{E}\left(Z_i(\mathbf{x})Z_j(\mathbf{x}')\right), \qquad \mathbf{x},\mathbf{x}' \in \mathbb{T}^{k,\ell},\ i,j = 1,\ldots,p,$$

with $\mathbb{E}$ denoting the mathematical expectation. Reciprocally, any covariance kernel on $\mathbb{T}^{k,\ell} \times \mathbb{T}^{k,\ell}$ is positive semidefinite.

Building covariance (positive semidefinite) kernels is mathematically challenging and simplifying assumptions are often required for modeling, estimation, and prediction (Chilès and Delfiner, 2012). Throughout, we assume that there exists a continuous (continuity is intended as pointwise and elementwise) mapping $\boldsymbol{C} : [-1,1]^2 \to \mathbb{R}^{p\times p}$ such that

$$\boldsymbol{K}(\mathbf{x}, \mathbf{x}') = \boldsymbol{C}(s, r), \quad \mathbf{x} = (x_1, y_1), \mathbf{x}' = (x_1', y_1'), \tag{2}$$

with $s := \langle x_1, x_1' \rangle_k, r := \langle y_1, y_1' \rangle_\ell$, for $x_1, x_1' \in \mathbb{S}^k$, $y_1, y_1' \in \mathbb{S}^\ell$ and where $\langle \cdot, \cdot \rangle_k$ and $\langle \cdot, \cdot \rangle_\ell$ are the usual dot products on $\mathbb{R}^{k+1}$ and $\mathbb{R}^{\ell+1}$, respectively. Note that s and r are the cosines of the geodesic distances taken over $\mathbb{S}^k$ and $\mathbb{S}^\ell$, respectively.

Hereinafter, we call $\boldsymbol{C}$ the componentwise isotropic part of the kernel $\boldsymbol{K}$, and denote $\mathcal{P}^p(\mathbb{T}^{k,\ell})$ the class of continuous mappings $\boldsymbol{C}$ satisfying identity (2). We use the analogous notation $\mathcal{P}^p(\mathbb{S}^k)$ for the class of continuous mappings $\boldsymbol{g} : [-1,1] \to \mathbb{R}^{p\times p}$ such that the kernel $(x, x') \mapsto \boldsymbol{g}(\langle x, x' \rangle_k)$, for $x, x' \in \mathbb{S}^k$, is positive semidefinite.

The componentwise isotropic part $\boldsymbol{C} \in \mathcal{P}^p(\mathbb{T}^{k,\ell})$ is separable if it can be written as the product of a function of s and a function of r:

$$\boldsymbol{C}(s, r) = \boldsymbol{C}_1(s)\, \boldsymbol{C}_2(r), \quad s, r \in [-1, 1].$$

A wealth of separable covariance kernels on the hypertorus $\mathbb{T}^{k,\ell}$ can be obtained by multiplying isotropic covariance kernels defined on the hyperspheres $\mathbb{S}^k$ and $\mathbb{S}^\ell$. We refer the reader to Huang et al. (2011), Gneiting (2013), Guinness and Fuentes (2016), Jeong et al. (2017), Xu (2018) and Lantuéjoul et al. (2019) for examples of scalar covariance kernels on hyperspheres, and to Porcu et al. (2016), Guella and Menegatto (2019), Bevilacqua et al. (2020) and Emery et al. (2022) for matrix-valued covariance kernels.

2.3 Spectral representations

Guella et al. (2016) proved that a continuous mapping $C : [-1,1]^2 \to \mathbb{R}$ with $C(1,1) < \infty$ belongs to the class $\mathcal{P}^1(\mathbb{T}^{k,\ell})$ if and only if

$$C(s, r) = \sum_{n=0}^{\infty} \sum_{m=0}^{\infty} b_{n,m}^{k,\ell} \mathcal{G}_n^{(k-1)/2}(s) \mathcal{G}_m^{(\ell-1)/2}(r), \quad s, r \in [-1, 1], \tag{3}$$

where $\mathcal{G}_n^\lambda$ stands for the Gegenbauer polynomial of degree n and order λ (for $\lambda > 0$) or the Chebychev polynomial of the first kind of degree n (for $\lambda = 0$) (Olver et al., 2010, Table 18.3.1), $b_{n,m}^{k,\ell} \geq 0$,

$$\sum_{n=0}^{\infty} \sum_{m=0}^{\infty} b_{n,m}^{k,\ell} \mathcal{G}_n^{(k-1)/2}(1) \mathcal{G}_m^{(\ell-1)/2}(1) < \infty$$

and

$$b_{n,m}^{k,\ell} \propto \int_{-1}^{1} C(s, r) \mathcal{G}_n^{(k-1)/2}(s) \mathcal{G}_m^{(\ell-1)/2}(r) (1 - s^2)^{k/2-1} (1 - r^2)^{\ell/2-1} \mathrm{d}s\, \mathrm{d}r.$$

A similar series expansion holds for the class $\mathcal{P}^1(\mathbb{S}^k)$, with the reader referred to Schoenberg (1942) for details.

The characterization of a p-variate isotropic covariance kernel on the k-dimensional sphere, $\boldsymbol{K} : \mathbb{S}^k \times \mathbb{S}^k \to \mathbb{R}^{p\times p}$, with $p > 1$ and $k > 0$, can be found in Yaglom (1987) and an alternative proof can be found in Bonfim and Menegatto (2016): the isotropic part $\boldsymbol{C} : [-1, 1] \to \mathbb{R}^{p\times p}$ of $\boldsymbol{K}$ belongs to the class $\mathcal{P}^p(\mathbb{S}^k)$ if and only if

$$\boldsymbol{C}(s) = \sum_{n=0}^{\infty} \boldsymbol{b}_n \mathcal{G}_n^{(k-1)/2}(s), \quad s \in [-1, 1], \tag{4}$$

where $\{\boldsymbol{b}_n\}_{n=0}^{\infty}$ is a sequence of symmetric positive semidefinite matrices of size $p \times p$ such that $\sum_{n=0}^{\infty} \boldsymbol{b}_n \mathcal{G}_n^{(k-1)/2}(1) < \infty$ (elementwise summation). This representation is a multivariate extension of Schoenberg's theorem (Schoenberg, 1942), reason for which the sequence $\{\boldsymbol{b}_n\}_{n=0}^{\infty}$ is known as the k-Schoenberg sequence of $\boldsymbol{C}$.

Using the techniques of Bonfim and Menegatto (2016) and Guella et al. (2016), one can infer the following result, which is an extension of (3) and agrees with the findings of Bachoc et al. (2021).

Theorem 1 *Let p a positive integer. A function $\boldsymbol{C} : [-1, 1]^2 \to \mathbb{R}^{p\times p}$ belongs to the class $\mathcal{P}^p(\mathbb{T}^{k,\ell})$ if and only if*

$$\boldsymbol{C}(s, r) = \sum_{n=0}^{\infty} \sum_{m=0}^{\infty} \boldsymbol{b}_{n,m}^{k,\ell} \mathcal{G}_n^{(k-1)/2}(s) \mathcal{G}_m^{(\ell-1)/2}(r), \quad s, r \in [-1, 1], \tag{5}$$

with $\{\boldsymbol{b}_{n,m}^{k,\ell}\}_{n,m=0}^{\infty}$ a sequence of symmetric positive semidefinite matrices of size $p\times p$ such that $\sum_{n=0}^{\infty} \sum_{m=0}^{\infty} \boldsymbol{b}_{n,m}^{k,\ell} \mathcal{G}_n^{(k-1)/2}(1) \mathcal{G}_m^{(\ell-1)/2}(1) < \infty$ (elementwise summation).

Hereinafter, we call $\boldsymbol{b}_{n,m}^{k,\ell}$ the (k, ℓ)-Schoenberg matrix of $\boldsymbol{C}$, and $\{\boldsymbol{b}_{n,m}^{k,\ell}\}_{n,m=0}^{\infty}$ the (k, ℓ)-Schoenberg sequence of $\boldsymbol{C}$.

3 Nonseparable covariance kernels on hypertori

Throughout this section, we consider $\lambda = \frac{k-1}{2}$ and $\mu = \frac{\ell-1}{2}$. For $n \in \mathbb{N}$ and $\nu \in \mathbb{R}$, we define

$$f(\nu, n) = \begin{cases} \frac{\nu \exp(-\pi\nu/2) \sinh(\pi\nu/2)}{2\pi} & \text{if } n \text{ is even} \\ \frac{\nu \exp(-\pi\nu/2) \cosh(\pi\nu/2)}{2\pi} & \text{if } n \text{ is odd,} \end{cases} \tag{6}$$

with sinh and cosh the hyperbolic sine and cosine, respectively. We also use the symbols and functions listed in Table 1.

Table 1: Symbols and ordinary and special functions

Notation	Function name
$\lfloor \cdot \rfloor$	Floor function
$\lvert \cdot \rvert$	Complex modulus
ι	Imaginary unit
$\mathcal{G}_n^{\nu}$	Gegenbauer (a.k.a. ultraspherical) polynomial of degree n and order ν
J_ν	Bessel function of the first kind of order ν
I_ν	Modified Bessel function of the first kind of order ν
Γ	Gamma function
$(\cdot)_k$	Pochhammer symbol, a.k.a. rising factorial
${}_0F_1$	Confluent hypergeometric function
${}_1F_1$	Kummer confluent hypergeometric function
${}_2F_1$	Gauss hypergeometric function

Next, we provide 26 parametric classes of nonseparable models in $\mathcal{P}^p(\mathbb{T}^{k,\ell})$, with $p > 0$, $k > 1$ and $\ell > 1$, together with their (k,ℓ)-Schoenberg sequences (Tables 2 to 11). At the end of each table, we provide sufficient conditions common to all the models of the table to be well-defined and positive semidefinite, i.e., to be valid covariance kernels.

3.1 Models based on elementary and gamma functions

The kernels $(s,r) \mapsto C(s,r)$ listed in Tables 2 and 3 are defined by sums, products and compositions of finitely many polynomial, rational, inverse trigonometric, logarithmic and exponential functions of the input parameters $\boldsymbol{a}$, $\boldsymbol{b}$, $\boldsymbol{\nu}$ and $\boldsymbol{\rho}$. Two other kernels also involving gamma functions are provided in Tables 4 and 5. Examples of graphical representations of the kernel marginals $s \mapsto C(s,1)$ and $r \mapsto C(1,r)$ are shown in Figure 1.

Table 2: Elementary covariance kernels, part 1.

Elementary model 1

Covariance kernel:

$$\boldsymbol{C} = \boldsymbol{\rho}\,(1 - 2r\exp(\boldsymbol{\nu}(s-\boldsymbol{a}) - \boldsymbol{b}) + \exp(2\boldsymbol{\nu}(s-\boldsymbol{a}) - 2\boldsymbol{b}))^{-\mu}$$

Schoenberg matrices:

$$\boldsymbol{b}_{n,m}^{k,\ell} = \boldsymbol{\rho}\,\exp(-m\boldsymbol{a}\boldsymbol{\nu} - m\boldsymbol{b})2^{\lambda}\Gamma(\lambda)(\lambda+n)(m\boldsymbol{\nu})^{-\lambda}I_{\lambda+n}(m\boldsymbol{\nu})$$

Elementary model 2

Covariance kernel:

$$\boldsymbol{C} = \boldsymbol{\rho}\,(1 - r\exp(\boldsymbol{\nu}(s-\boldsymbol{a}) - \boldsymbol{b}))\,(1 - 2r\exp(\boldsymbol{\nu}(s-\boldsymbol{a}) - \boldsymbol{b}) + \exp(2\boldsymbol{\nu}(s-\boldsymbol{a}) - 2\boldsymbol{b}))^{-\boldsymbol{\nu}-1}$$

Schoenberg matrices:

$$\boldsymbol{b}_{n,m}^{k,\ell} = \boldsymbol{\rho}\frac{m+2\mu}{4\mu}\exp(-m\boldsymbol{a}\boldsymbol{\nu} - m\boldsymbol{b})\,2^{\lambda}\Gamma(\lambda)(\lambda+n)(m\boldsymbol{\nu})^{-\lambda}I_{\lambda+n}(m\boldsymbol{\nu})$$

To be continued

Table 2 (continued)

Elementary model 3

Covariance kernel:

$$\boldsymbol{C} = \boldsymbol{\rho}\, 2^{\mu-1/2}(1 - 2r\exp(\boldsymbol{\nu}(s-\boldsymbol{a})-\boldsymbol{b}) + \exp(2\boldsymbol{\nu}(s-\boldsymbol{a})-2\boldsymbol{b}))^{-1/2} \times \left(1 - r\exp(\boldsymbol{\nu}(s-\boldsymbol{a})-\boldsymbol{b}) + \sqrt{1-2r\exp(\boldsymbol{\nu}(s-\boldsymbol{a})-\boldsymbol{b})+\exp(2\boldsymbol{\nu}(s-\boldsymbol{a})-2\boldsymbol{b})}\right)^{1/2-\mu}$$

Schoenberg matrices:

$$\boldsymbol{b}_{n,m}^{k,\ell} = \boldsymbol{\rho}\,\frac{(\mu+\frac{1}{2})_m}{(2\mu)_m}\exp(-m\boldsymbol{a}\boldsymbol{\nu} - m\boldsymbol{b})2^{\lambda}\Gamma(\lambda)(\lambda+n)(m\boldsymbol{\nu})^{-\lambda}\, I_{\lambda+n}(m\,\boldsymbol{\nu})$$

Elementary model 4

Covariance kernel:

$$\boldsymbol{C} = \boldsymbol{\rho}\,(1 + 2r\exp(\boldsymbol{\nu}(s-\boldsymbol{a})-\boldsymbol{b}) + \exp(2\boldsymbol{\nu}(s-\boldsymbol{a})-2\boldsymbol{b}))^{\kappa/2} \times \mathcal{G}_{\kappa}^{\mu}\left(\frac{r+\exp(\boldsymbol{\nu}(s-\boldsymbol{a})-\boldsymbol{b})}{\sqrt{1+2r\exp(\boldsymbol{\nu}(s-\boldsymbol{a})-\boldsymbol{b})+\exp(2\boldsymbol{\nu}(s-\boldsymbol{a})-2\boldsymbol{b})}}\right)$$

Schoenberg matrices:

$$\boldsymbol{b}_{n,m}^{k,\ell} = \begin{cases} \boldsymbol{0} & \text{if } m > \kappa \\ \boldsymbol{\rho}\,\dfrac{\exp(-(\kappa-m)(\boldsymbol{a}\boldsymbol{\nu}+\boldsymbol{b}))\,\Gamma(\kappa+2\mu)}{(\kappa-m)!\,\Gamma(m+2\mu)}\,2^{\lambda}\,\Gamma(\lambda)(\lambda+n)((\kappa-m)\boldsymbol{\nu})^{-\lambda}\, I_{\lambda+n}((\kappa-m)\boldsymbol{\nu}) & \text{otherwise} \end{cases}$$

Elementary model 5

Covariance kernel:

$$\boldsymbol{C} = \boldsymbol{\rho}\,(1 + 2r\exp(\boldsymbol{\nu}(s-\boldsymbol{a})-\boldsymbol{b}) + \exp(2\boldsymbol{\nu}(s-\boldsymbol{a})-2\boldsymbol{b}))^{\kappa/2} \times \mathcal{G}_{\kappa}^{\mu}\left(\frac{1+r\exp(\boldsymbol{\nu}(s-\boldsymbol{a})-\boldsymbol{b})}{\sqrt{1+2r\exp(\boldsymbol{\nu}(s-\boldsymbol{a})-\boldsymbol{b})+\exp(2\boldsymbol{\nu}(s-\boldsymbol{a})-2\boldsymbol{b})}}\right)$$

Schoenberg matrices:

$$\boldsymbol{b}_{n,m}^{k,\ell} = \begin{cases} \boldsymbol{0} & \text{if } m > \kappa \\ \boldsymbol{\rho}\,\dfrac{\exp(-m\boldsymbol{a}\boldsymbol{\nu}-m\boldsymbol{b})\,\Gamma(\kappa+2\mu)}{(\kappa-m)!\,\Gamma(m+2\mu)}\,2^{\lambda}\,\Gamma(\lambda)(\lambda+n)(m\boldsymbol{\nu})^{-\lambda}\, I_{\lambda+n}(m\boldsymbol{\nu}) & \text{otherwise} \end{cases}$$

Sufficient conditions for convergence:

$\kappa \in \mathbb{N}$, $\boldsymbol{\nu}$ and $\boldsymbol{b} + (\boldsymbol{a}-1)\boldsymbol{\nu}$ with entries in $(0,\infty)$, and $\boldsymbol{\rho}$ with entries in $\mathbb{R}$

Sufficient conditions for positive semidefiniteness:

(A) (1) $\boldsymbol{a}$ is conditionally negative semidefinite
(2) $\boldsymbol{b}$ is conditionally negative semidefinite
(3) $\boldsymbol{\nu} = \nu\boldsymbol{1}$
(4) $\boldsymbol{\rho}$ is positive semidefinite

or

(B) (1) $-\boldsymbol{a}$ is positive semidefinite
(2) $\boldsymbol{b}$ is conditionally negative semidefinite
(3) $\boldsymbol{\nu}$ is positive semidefinite
(4) $\boldsymbol{\rho}$ is positive semidefinite

Table 3: Elementary covariance kernels, part 2.

Elementary model 6

Covariance kernel:

$$\boldsymbol{C} = \boldsymbol{\rho}(1 - 2\exp(-\boldsymbol{\nu}(\arccos(s) + \boldsymbol{a}))r + \exp(-2\boldsymbol{\nu}(\arccos(s) + \boldsymbol{a})))^{-\mu}$$

Schoenberg matrices:

$$\boldsymbol{b}_{n,m}^{k,\ell} = \boldsymbol{\rho}\exp(-m\boldsymbol{a}\boldsymbol{\nu}) f(m\boldsymbol{\nu}, n)\,(\lambda + n)\,\Gamma(\lambda)\,\Gamma(\lambda+1)\,\frac{\left|\Gamma(\frac{n+\iota m\boldsymbol{\nu}}{2})\right|^2}{\left|\Gamma(\lambda+1+\frac{n+\iota m\boldsymbol{\nu}}{2})\right|^2}$$

Elementary model 7

Covariance kernel:

$$\boldsymbol{C} = \boldsymbol{\rho}(1 - \exp(-\boldsymbol{\nu}(\arccos(s) + \boldsymbol{a}))r)(1 - 2\exp(-\boldsymbol{\nu}(\arccos(s) + \boldsymbol{a}))r + \exp(-2\boldsymbol{\nu}(\arccos(s) + \boldsymbol{a})))^{-\mu-1}$$

Schoenberg matrices:

$$\boldsymbol{b}_{n,m}^{k,\ell} = \boldsymbol{\rho}\,\frac{(m+2\mu)}{4\mu}\exp(-m\boldsymbol{a}\boldsymbol{\nu}) f(m\boldsymbol{\nu}, n)\,(\lambda + n)\,\Gamma(\lambda)\,\Gamma(\lambda+1)\,\frac{\left|\Gamma(\frac{n+\iota m\boldsymbol{\nu}}{2})\right|^2}{\left|\Gamma(\lambda+1+\frac{n+\iota m\boldsymbol{\nu}}{2})\right|^2}$$

Elementary model 8

Covariance kernel:

$$\boldsymbol{C} = \boldsymbol{\rho}\,2^{\mu-1/2}(1 - 2\exp(-\boldsymbol{\nu}(\arccos(s) + \boldsymbol{a}))r + \exp(-2\boldsymbol{\nu}(\arccos(s) + \boldsymbol{a})))^{-1/2}$$
$$\times\left(1 - \exp(-\boldsymbol{\nu}(\arccos(s) + \boldsymbol{a}))r + \sqrt{1 - 2\exp(-\boldsymbol{\nu}(\arccos(s) + \boldsymbol{a}))r + \exp(-2\boldsymbol{\nu}(\arccos(s) + \boldsymbol{a}))}\right)^{1/2-\mu}$$

Schoenberg matrices:

$$\boldsymbol{b}_{n,m}^{k,\ell} = \boldsymbol{\rho}\,\frac{(\mu+\frac{1}{2})_m}{(2\mu)_m}\exp(-m\boldsymbol{a}\boldsymbol{\nu}) f(m\boldsymbol{\nu}, n)\,(\lambda + n)\,\Gamma(\lambda)\,\Gamma(\lambda+1)\,\frac{\left|\Gamma(\frac{n+\iota m\boldsymbol{\nu}}{2})\right|^2}{\left|\Gamma(\lambda+1+\frac{n+\iota m\boldsymbol{\nu}}{2})\right|^2}$$

Elementary model 9

Covariance kernel:

$$\boldsymbol{C} = \boldsymbol{\rho}\,(1 + 2\exp(-\boldsymbol{\nu}(\arccos(s) + \boldsymbol{a}))r + \exp(-2\boldsymbol{\nu}(\arccos(s) + \boldsymbol{a})))^{\kappa/2}$$
$$\times\,\mathcal{G}_\kappa^\mu\left(\frac{r + \exp(-\boldsymbol{\nu}(\arccos(s) + \boldsymbol{a}))}{\sqrt{1 + 2\exp(-\boldsymbol{\nu}(\arccos(s) + \boldsymbol{a}))r + \exp(-2\boldsymbol{\nu}(\arccos(s) + \boldsymbol{a}))}}\right)$$

Schoenberg matrices:

$$\boldsymbol{b}_{n,m}^{k,\ell} = \begin{cases} \boldsymbol{0}, & \text{if } m > \kappa \\ \boldsymbol{\rho}\,\dfrac{\Gamma(\kappa+2\mu)\exp(-(m-\kappa)\boldsymbol{a}\boldsymbol{\nu})}{(\kappa-m)!\,\Gamma(m+2\mu)} & \\ \quad\times f((\kappa-m)\boldsymbol{\nu}, n)(\lambda+n)\Gamma(\lambda)\Gamma(\lambda+1)\dfrac{\left|\Gamma(\frac{n+\iota(\kappa-m)\boldsymbol{\nu}}{2})\right|^2}{\left|\Gamma(\lambda+1+\frac{n+\iota(\kappa-m)\boldsymbol{\nu}}{2})\right|^2}, & \text{otherwise} \end{cases}$$

Elementary model 10

Covariance kernel:

$$\boldsymbol{C} = \boldsymbol{\rho}\,(1 + 2\exp(-\boldsymbol{\nu}(\arccos(s) + \boldsymbol{a}))r + \exp(-2\boldsymbol{\nu}(\arccos(s) + \boldsymbol{a})))^{\kappa/2}$$
$$\times\,\mathcal{G}_\kappa^\mu\left(\frac{1 + \exp(-\boldsymbol{\nu}(\arccos(s) + \boldsymbol{a}))r}{\sqrt{1 + 2\exp(-\boldsymbol{\nu}(\arccos(s) + \boldsymbol{a}))r + \exp(-2\boldsymbol{\nu}(\arccos(s) + \boldsymbol{a}))}}\right)$$

To be continued

Table 3 (continued)

Schoenberg matrices:

$$\boldsymbol{b}_{n,m}^{k,\ell} = \begin{cases} \mathbf{0}, & \text{if } m > \kappa \\ \boldsymbol{\rho} \dfrac{\Gamma(\kappa+2\mu)\exp(-m\boldsymbol{a}\boldsymbol{\nu})}{(\kappa-m)!\,\Gamma(m+2\mu)} f(m\boldsymbol{\nu},n)\,(\lambda+n)\,\Gamma(\lambda)\,\Gamma(\lambda+1)\,\dfrac{\left|\Gamma(\frac{n+\iota m\boldsymbol{\nu}}{2})\right|^2}{\left|\Gamma(\lambda+1+\frac{n+\iota m\boldsymbol{\nu}}{2})\right|^2}, & \text{otherwise} \end{cases}$$

Sufficient conditions for convergence:

$\kappa \in \mathbb{N}$, $\boldsymbol{a}$ and $\boldsymbol{\nu}$ with entries in $(0,\infty)$, and $\boldsymbol{\rho}$ with entries in $\mathbb{R}$

Sufficient conditions for positive semidefiniteness:

(A) (1) $\boldsymbol{a}$ is conditionally negative semidefinite
(2) $\boldsymbol{\nu} = \nu\mathbf{1}$
(3) $\boldsymbol{\rho}$ is positive semidefinite
or
(B) (1) $\boldsymbol{a} = a\mathbf{1}$
(2) $\boldsymbol{\nu}^2$ is conditionally negative semidefinite
(3) $\boldsymbol{\rho} f(\boldsymbol{\nu},0)$ is positive semidefinite
(4) $\boldsymbol{\rho} f(\boldsymbol{\nu},1)$ is positive semidefinite

Table 4: Covariance kernels involving elementary and gamma functions, part 1.

Special model 1

Covariance kernel:

$$\boldsymbol{C} = \frac{\boldsymbol{\rho}\Gamma(2\mu)\Gamma(\boldsymbol{\kappa}+1)}{\Gamma(\boldsymbol{\kappa}+2\mu)(1-2r\exp(\boldsymbol{\nu}(s-\boldsymbol{a})-\boldsymbol{b})+\exp(2\boldsymbol{\nu}(s-\boldsymbol{a})-2\boldsymbol{b}))^{\mu+\boldsymbol{\kappa}/2}} \times \mathcal{G}_{\boldsymbol{\kappa}}^{\mu}\left(\frac{1-r\exp(\boldsymbol{\nu}(s-\boldsymbol{a})-\boldsymbol{b})}{\sqrt{1-2r\exp(\boldsymbol{\nu}(s-\boldsymbol{a})-\boldsymbol{b})+\exp(2\boldsymbol{\nu}(s-\boldsymbol{a})-2\boldsymbol{b})}}\right)$$

Schoenberg matrices:

$$\boldsymbol{b}_{n,m}^{k,\ell} = \boldsymbol{\rho}\,\frac{(\boldsymbol{\kappa}+2\mu)_m\,\exp(-m\boldsymbol{a}\,\boldsymbol{\nu}-m\boldsymbol{b})}{(2\mu)_m}\,2^{\lambda}\,\Gamma(\lambda)\,(\lambda+n)\,(m\boldsymbol{\nu})^{-\lambda}I_{\lambda+n}(m\,\boldsymbol{\nu})$$

Sufficient conditions for convergence:

$\boldsymbol{\nu}$ and $\boldsymbol{b}+(\boldsymbol{a}-1)\boldsymbol{\nu}$ with entries in $(0,\infty)$, $\boldsymbol{\kappa}$ with entries in $\mathbb{N}$, and $\boldsymbol{\rho}$ with entries in $\mathbb{R}$

Sufficient conditions for positive semidefiniteness:

To be continued

Table 4 (continued)

(A) (1) $\boldsymbol{a}$ is conditionally negative semidefinite
(2) $\boldsymbol{b}$ is conditionally negative semidefinite
(3) $\boldsymbol{\nu} = \nu \mathbf{1}$
(4) $\boldsymbol{\kappa}$ is positive semidefinite
(5) $\boldsymbol{\rho}$ is positive semidefinite
or
(B) (1) $-\boldsymbol{a}$ is positive semidefinite
(2) $\boldsymbol{b}$ is conditionally negative semidefinite
(3) $\boldsymbol{\nu}$ is positive semidefinite
(4) $\boldsymbol{\kappa}$ is positive semidefinite
(5) $\boldsymbol{\rho}$ is positive semidefinite

Table 5: Covariance kernels involving elementary and gamma functions, part 2.

Special model 2

Covariance kernel:

$$\boldsymbol{C} = \frac{\boldsymbol{\rho}\, \Gamma(2\mu)\Gamma(\boldsymbol{\kappa}+1)}{\Gamma(\boldsymbol{\kappa}+2\mu)(1-2\exp(-\boldsymbol{\nu}(\arccos(s)+\boldsymbol{a}))r+\exp(-2\boldsymbol{\nu}(\arccos(s)+\boldsymbol{a})))^{\mu+\boldsymbol{\kappa}/2}} \times \mathcal{G}_{\boldsymbol{\kappa}}^{\mu}\left(\frac{1-\exp(-\boldsymbol{\nu}(\arccos(s)+\boldsymbol{a}))r}{\sqrt{1-2\exp(-\boldsymbol{\nu}(\arccos(s)+\boldsymbol{a}))r+\exp(-2\boldsymbol{\nu}(\arccos(s)+\boldsymbol{a}))}}\right)$$

Schoenberg matrices:

$$\boldsymbol{b}_{n,m}^{k,\ell} = \boldsymbol{\rho}\, \frac{(2\mu+\boldsymbol{\kappa})_m \exp(-m\boldsymbol{a}\boldsymbol{\nu})}{(2\mu)_m}\, f(m\boldsymbol{\nu}, n)\, (\lambda+n)\, \Gamma(\lambda)\, \Gamma(\lambda+1)\, \frac{\left|\Gamma(\frac{n+\iota m\boldsymbol{\nu}}{2})\right|^2}{\left|\Gamma(\lambda+1+\frac{n+\iota m\boldsymbol{\nu}}{2})\right|^2}$$

Sufficient conditions for convergence:

$\boldsymbol{a}$ and $\boldsymbol{\nu}$ with entries in $(0,\infty)$, $\boldsymbol{\kappa}$ with entries in $\mathbb{N}$ and $\boldsymbol{\rho}$ with entries in $\mathbb{R}$

Sufficient conditions for positive semidefiniteness:

To be continued

Table 5 (continued)

(A)	(1)	$\boldsymbol{a}$ is conditionally negative semidefinite
	(2)	$\boldsymbol{\nu} = \nu\mathbf{1}$
	(3)	$\boldsymbol{\kappa}$ is positive semidefinite
	(4)	$\boldsymbol{\rho}$ is positive semidefinite
	or	
(B)	(1)	$\boldsymbol{a} = a\mathbf{1}$
	(2)	$\boldsymbol{\nu}^2$ is conditionally negative semidefinite
	(3)	$\boldsymbol{\kappa}$ is positive semidefinite
	(4)	$\boldsymbol{\rho} f(\boldsymbol{\nu}, 0)$ is positive semidefinite
	(5)	$\boldsymbol{\rho} f(\boldsymbol{\nu}, 1)$ is positive semidefinite

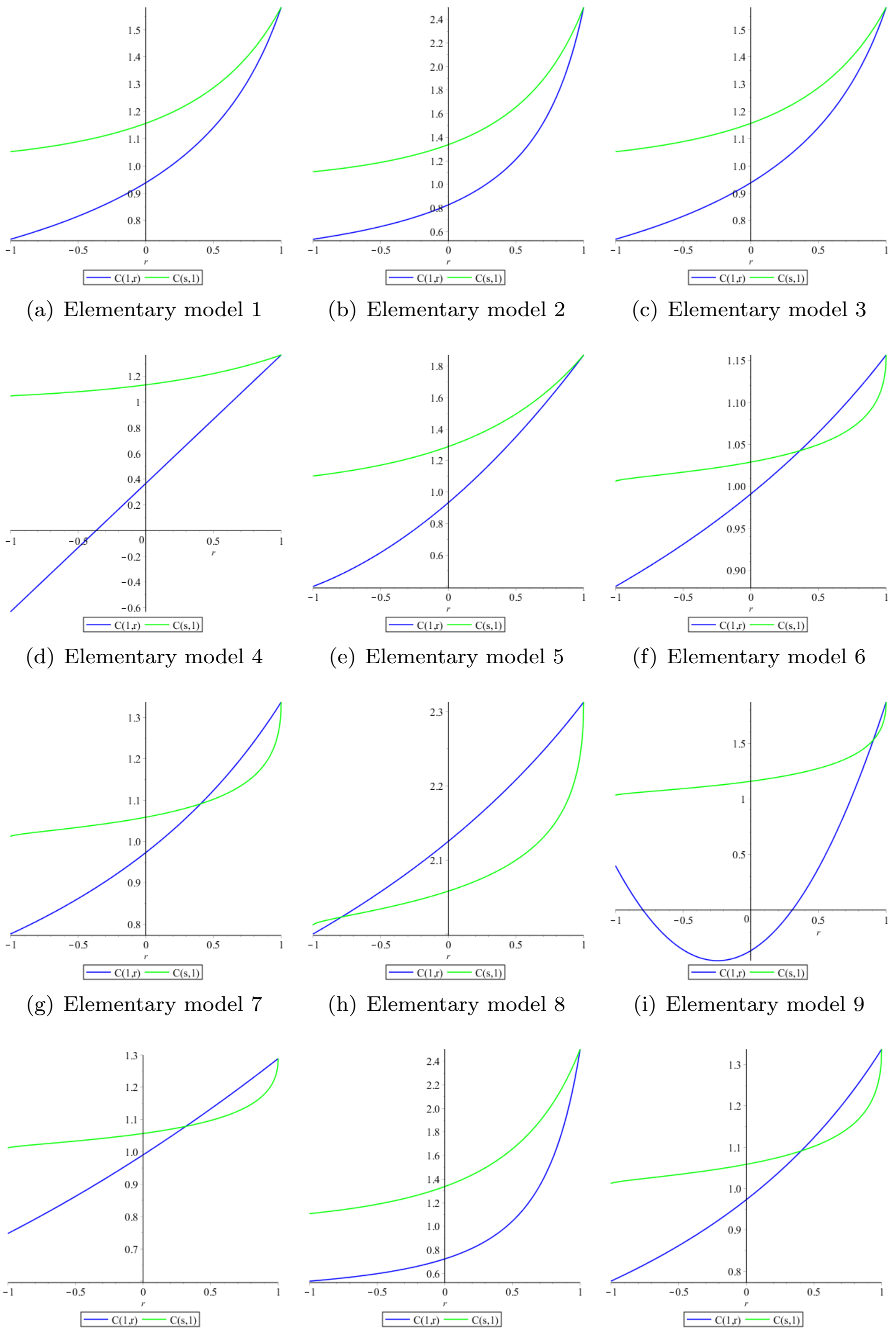

(a) Elementary model 1 (b) Elementary model 2 (c) Elementary model 3

(d) Elementary model 4 (e) Elementary model 5 (f) Elementary model 6

(g) Elementary model 7 (h) Elementary model 8 (i) Elementary model 9

(j) Elementary model 10 (k) Special model 1 (l) Special model 2

Fig. 1: Examples of elementary models and special models involving elementary and gamma functions. Representation of the marginals $s \mapsto C(s,1)$ (green) and $r \mapsto C(1,r)$ (blue) for s and r ranging from -1 to 1

3.2 Bessel and hypergeometric models

Tables 6 to 11 list covariance kernels involving Bessel or hypergeometric functions, while Figures 2 and 3 show examples of kernel marginals.

Table 6: Bessel covariance kernels, part 1.

Bessel model 1

Covariance kernel:

$$\boldsymbol{C} = \boldsymbol{\rho}\, \Gamma(\mu + \tfrac{1}{2}) \exp(r \exp(\boldsymbol{\nu}(s - \boldsymbol{a}) - \boldsymbol{b})) \\ \times \left(\tfrac{1}{2} \exp(\boldsymbol{\nu}(s - \boldsymbol{a}) - \boldsymbol{b})(1 - r^2)^{1/2}\right)^{\frac{1}{2}-\mu} J_{\mu-\frac{1}{2}}(\exp(\boldsymbol{\nu}(s - \boldsymbol{a}) - \boldsymbol{b})(1 - r^2)^{1/2})$$

Schoenberg matrices:

$$\boldsymbol{b}_{n,m}^{k,\ell} = \boldsymbol{\rho}\, \frac{\exp(-m\boldsymbol{a}\boldsymbol{\nu} - m\boldsymbol{b})}{(2\mu)_m} 2^\lambda \Gamma(\lambda)(\lambda + n)(m\boldsymbol{\nu})^{-\lambda} I_{\lambda+n}(m\boldsymbol{\nu})$$

Bessel model 2

Covariance kernel:

$$\boldsymbol{C} = \boldsymbol{\rho} \left(\tfrac{1}{2} \exp(\boldsymbol{\nu}(s - \boldsymbol{a}) - \boldsymbol{b})(1 - r^2)^{1/2}\right)^{\frac{1}{2}-\mu} \\ \times J_{\mu-\frac{1}{2}}\left(\sqrt{2 \exp(\boldsymbol{\nu}(s - \boldsymbol{a}) - \boldsymbol{b})(1 - r)}\right) I_{\mu-\frac{1}{2}}\left(\sqrt{2 \exp(\boldsymbol{\nu}(s - \boldsymbol{a}) - \boldsymbol{b})(1 + r)}\right)$$

Schoenberg matrices:

$$\boldsymbol{b}_{n,m}^{k,\ell} = \boldsymbol{\rho}\, \frac{\exp(-m\boldsymbol{a}\boldsymbol{\nu} - m\boldsymbol{b})}{\Gamma(\mu + \frac{1}{2})\Gamma(\mu + m + \frac{1}{2})(2\mu)_m} 2^\lambda \Gamma(\lambda)(\lambda + n)(m\boldsymbol{\nu})^{-\lambda} I_{\lambda+n}(m\boldsymbol{\nu})$$

Sufficient conditions for convergence:

$\boldsymbol{\nu}$ and $\boldsymbol{b} + (\boldsymbol{a} - 1)\boldsymbol{\nu}$ with entries in $(0, \infty)$, and $\boldsymbol{\rho}$ with entries in $\mathbb{R}$

Sufficient conditions for positive semidefiniteness:

(A) (1) $\boldsymbol{a}$ is conditionally negative semidefinite
(2) $\boldsymbol{b}$ is conditionally negative semidefinite
(3) $\boldsymbol{\nu} = \nu\mathbf{1}$
(4) $\boldsymbol{\rho}$ is positive semidefinite
or
(B) (1) $-\boldsymbol{a}$ is positive semidefinite
(2) $\boldsymbol{b}$ is conditionally negative semidefinite
(3) $\boldsymbol{\nu}$ is positive semidefinite
(4) $\boldsymbol{\rho}$ is positive semidefinite

Table 7: Bessel covariance kernels, part 2.

Bessel model 3

Covariance kernel:

$$\boldsymbol{C} = \boldsymbol{\rho}\, \Gamma(\mu + \tfrac{1}{2}) \exp(e^{-\boldsymbol{\nu}(\arccos(s)+\boldsymbol{a})} r) \left(\tfrac{1}{2} e^{-\boldsymbol{\nu}(\arccos(s)+\boldsymbol{a})} (1-r^2)^{1/2}\right)^{\frac{1}{2}-\mu} J_{\mu-\frac{1}{2}} \left(e^{-\boldsymbol{\nu}(\arccos(s)+\boldsymbol{a})} (1-r^2)^{1/2}\right)$$

Schoenberg matrices:

$$\boldsymbol{b}_{n,m}^{k,\ell} = \boldsymbol{\rho}\, \frac{\exp(-m\boldsymbol{a}\boldsymbol{\nu})}{(2\mu)_m} f(m\boldsymbol{\nu}, n) \Gamma(\lambda)(\lambda+n) \frac{\left|\Gamma(\frac{n+\iota m\boldsymbol{\nu}}{2})\right|^2}{\left|\Gamma(\lambda+1+\frac{n+\iota m\boldsymbol{\nu}}{2})\right|^2}$$

Bessel model 4

Covariance kernel:

$$\boldsymbol{C} = \boldsymbol{\rho} \left(\tfrac{1}{2} \exp(-\boldsymbol{\nu}(\arccos(s)+\boldsymbol{a}))(1-r^2)^{1/2}\right)^{\frac{1}{2}-\mu}$$
$$\times J_{\mu-\frac{1}{2}} \left(\sqrt{2\exp(-\boldsymbol{\nu}(\arccos(s)+\boldsymbol{a}))(1-r)}\right) I_{\mu-\frac{1}{2}} \left(\sqrt{2\exp(-\boldsymbol{\nu}(\arccos(s)+\boldsymbol{a}))(1+r)}\right)$$

Schoenberg matrices:

$$\boldsymbol{b}_{n,m}^{k,\ell} = \boldsymbol{\rho}\, \frac{\exp(-m\boldsymbol{a}\boldsymbol{\nu})}{\Gamma(\mu+\frac{1}{2})\Gamma(\mu+m+\frac{1}{2})(2\mu)_m} f(m\boldsymbol{\nu}, n)(\lambda+n)\Gamma(\lambda)\Gamma(\lambda+1) \frac{\left|\Gamma(\frac{n+\iota m\boldsymbol{\nu}}{2})\right|^2}{\left|\Gamma(\lambda+1+\frac{n+\iota m\boldsymbol{\nu}}{2})\right|^2}$$

Sufficient conditions for convergence:

$\boldsymbol{a}$ and $\boldsymbol{\nu}$ with entries in $(0,\infty)$, and $\boldsymbol{\rho}$ with entries in $\mathbb{R}$

Sufficient conditions for positive semidefiniteness:

(A) (1) $\boldsymbol{a}$ is conditionally negative semidefinite
(2) $\boldsymbol{\nu} = \nu\boldsymbol{1}$
(3) $\boldsymbol{\rho}$ is positive semidefinite
or
(B) (1) $\boldsymbol{a} = a\boldsymbol{1}$
(2) $\boldsymbol{\nu}^2$ is conditionally negative semidefinite
(3) $\boldsymbol{\rho} f(\boldsymbol{\nu}, 0)$ is positive semidefinite
(4) $\boldsymbol{\rho} f(\boldsymbol{\nu}, 1)$ is positive semidefinite

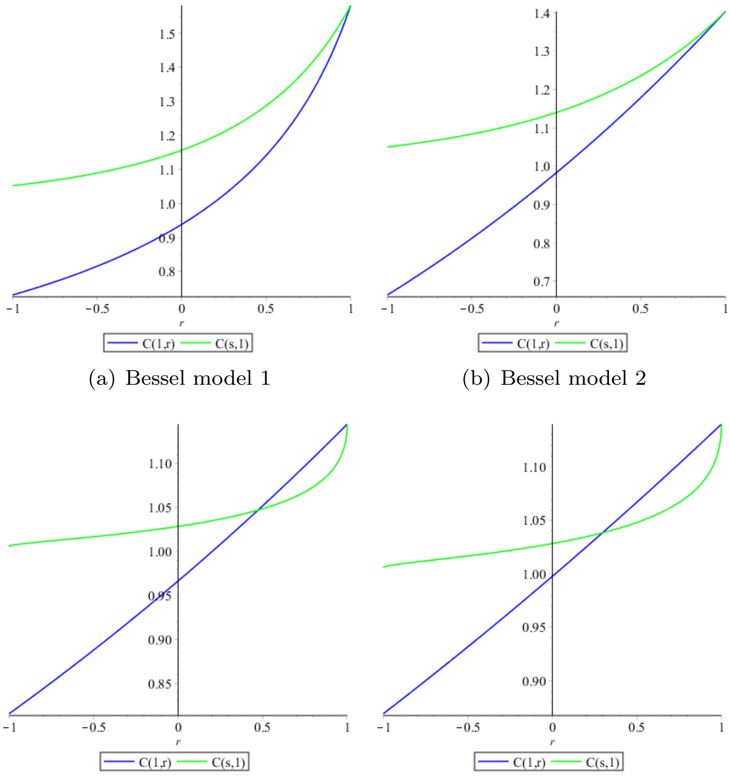

(a) Bessel model 1 (b) Bessel model 2

(c) Bessel model 3 (d) Bessel model 4

Fig. 2: Examples of Bessel models. Representation of the marginals $s \mapsto C(s,1)$ (green) and $r \mapsto C(1,r)$ (blue) for s and r ranging from -1 to 1

Table 8: Hypergeometric covariance kernels, part 1.

Hypergeometric model 1
Covariance kernel: $\boldsymbol{C} = \dfrac{\boldsymbol{\rho}}{(1-\exp(-\nu(\arccos(s)+\boldsymbol{a}))r)^{\boldsymbol{\kappa}}}\,{}_2F_1\left(\dfrac{\boldsymbol{\kappa}}{2},\dfrac{\boldsymbol{\kappa}+1}{2};\mu+\dfrac{1}{2};-\dfrac{\exp(-2\nu(\arccos(s)+\boldsymbol{a}))(1-r^2)}{(1-\exp(-\nu(\arccos(s)+\boldsymbol{a}))r)^2}\right)$
Schoenberg matrices: $\boldsymbol{b}_{n,m}^{k,\ell} = \boldsymbol{\rho}\,\dfrac{\exp(-\boldsymbol{a}m\nu)(\boldsymbol{\kappa})_m}{(2\mu)_m}f(m\nu,n)(\lambda+n)\Gamma(\lambda)\Gamma(\lambda+1)\dfrac{\left\|\Gamma(\frac{n+\iota m\nu}{2})\right\|^2}{\left\|\Gamma(\lambda+1+\frac{n+\iota m\nu}{2})\right\|^2}$
Hypergeometric model 2

To be continued

Table 8 (continued)

Covariance kernel:

$$\boldsymbol{C} = \frac{\boldsymbol{\rho}}{(1-\exp(\nu(s-1-\boldsymbol{a}))r)^{\boldsymbol{\kappa}}}\,{}_2F_1\left(\frac{\boldsymbol{\kappa}}{2}, \frac{\boldsymbol{\kappa}+1}{2}; \mu+\frac{1}{2}; -\frac{\exp(2\nu(s-1-\boldsymbol{a}))(1-r^2)}{(1-\exp(\nu(s-1-\boldsymbol{a}))r)^2}\right)$$

Schoenberg matrices:

$$\boldsymbol{b}_{n,m}^{k,\ell} = \boldsymbol{\rho}\,\frac{\exp(-(1+\boldsymbol{a})m\nu)(\boldsymbol{\kappa})_m}{(2\mu)_m} 2^{\lambda}(\lambda+n)(m\nu)^{-\lambda}\Gamma(\lambda)I_{\lambda+n}(m\nu),$$

Sufficient conditions for convergence:

$\boldsymbol{a}$ with entries in $(\frac{\ln(2)}{2\nu}, \infty)$, $\nu > 0$ and $\boldsymbol{\rho}$ and $\boldsymbol{\kappa}$ with entries in $\mathbb{R}$

Sufficient conditions for positive semidefiniteness:

(1) $\boldsymbol{a}$ is conditionally negative semidefinite
(2) $\boldsymbol{\rho}$ is positive semidefinite
(3) $\boldsymbol{\kappa}$ is positive semidefinite

Table 9: Hypergeometric covariance kernels, part 2.

Hypergeometric model 3

Covariance kernel:

$$\boldsymbol{C} = \boldsymbol{\rho}\,{}_2F_1\left(\boldsymbol{\kappa}, 2\mu-\boldsymbol{\kappa}; \mu+\tfrac{1}{2}; \frac{1-e^{-\nu(\arccos(s)+\boldsymbol{a})}-\sqrt{1-2e^{-\nu(\arccos(s)+\boldsymbol{a})}r+e^{-2\nu(\arccos(s)+\boldsymbol{a})}}}{2}\right)$$
$$\times\,{}_2F_1\left(\boldsymbol{\kappa}, 2\mu-\boldsymbol{\kappa}; \mu+\tfrac{1}{2}; \frac{1+e^{-\nu(\arccos(s)+\boldsymbol{a})}-\sqrt{1-2e^{-\nu(\arccos(s)+\boldsymbol{a})}r+e^{-2\nu(\arccos(s)+\boldsymbol{a})}}}{2}\right)$$

Schoenberg matrices:

$$\boldsymbol{b}_{n,m}^{k,\ell} = \boldsymbol{\rho}\,\frac{\exp(-\boldsymbol{a}m\nu)(2\mu-\boldsymbol{\kappa})_m(\boldsymbol{\kappa})_m}{(2\mu)_m(\mu+\frac{1}{2})_m} f(m\nu,n)(\lambda+n)\Gamma(\lambda)\Gamma(\lambda+1)\frac{\left|\Gamma(\frac{n+\iota m\nu}{2})\right|^2}{\left|\Gamma(\lambda+1+\frac{n+\iota m\nu}{2})\right|^2}$$

Hypergeometric model 4

Covariance kernel:

$$\boldsymbol{C} = \boldsymbol{\rho}\,{}_2F_1\left(\boldsymbol{\kappa}, 2\mu-\boldsymbol{\kappa}; \mu+\tfrac{1}{2}; \tfrac{1-\exp(\nu(s-1-\boldsymbol{a}))-\sqrt{1-2\exp(\nu(s-1-\boldsymbol{a}))r+\exp(2\nu(s-1-\boldsymbol{a}))}}{2}\right)$$
$$\times\,{}_2F_1\left(\boldsymbol{\kappa}, 2\mu-\boldsymbol{\kappa}; \mu+\tfrac{1}{2}; \tfrac{1+\exp(\nu(s-1-\boldsymbol{a}))-\sqrt{1-2\exp(\nu(s-1-\boldsymbol{a}))r+\exp(2\nu(s-1-\boldsymbol{a}))}}{2}\right)$$

Schoenberg matrices:

To be continued

Table 9 (continued)

$$\boldsymbol{b}_{n,m}^{k,\ell} = \boldsymbol{\rho}\, \frac{\exp(-(1+\boldsymbol{a})m\nu)(2\mu-\boldsymbol{\kappa})_m(\boldsymbol{\kappa})_m}{(2\mu)_m(\mu+\frac{1}{2})_m}\, 2^{\lambda}(\lambda+n)(m\nu)^{-\lambda}\Gamma(\lambda)I_{\lambda+n}(m\nu),$$

Sufficient conditions for convergence:

$\boldsymbol{a}$ with entries in $(0,\infty)$, $\nu > 0$ and $\boldsymbol{\rho}$ and $2\mu\boldsymbol{\kappa}-\boldsymbol{\kappa}^2$ with entries in $\mathbb{R}$

Sufficient conditions for positive semidefiniteness:

(1) $\boldsymbol{a}$ is conditionally negative semidefinite
(2) $\boldsymbol{\rho}$ is positive semidefinite
(3) $2\mu\boldsymbol{\kappa}-\boldsymbol{\kappa}^2$ is positive semidefinite

Table 10: Hypergeometric covariance kernels, part 3.

Hypergeometric model 5

Covariance kernel:

$$\boldsymbol{C} = \frac{\boldsymbol{\rho}}{(1-2\boldsymbol{b}\exp(-\nu(\arccos(s)+\boldsymbol{a}))r+\exp(-2\nu(\arccos(s)+\boldsymbol{a})))^{\mu}} \times {}_2F_1\left(\frac{\mu}{2},\frac{\mu+1}{2};\mu+\frac{1}{2};\frac{4\exp(-2\nu(\arccos(s)+\boldsymbol{a}))(1-\boldsymbol{b}^2)(1-r^2)}{(1-2\boldsymbol{b}\exp(-\nu(\arccos(s)+\boldsymbol{a}))r+\exp(-2\nu(\arccos(s)+\boldsymbol{a})))^2}\right)$$

Schoenberg matrices:

$$\boldsymbol{b}_{n,m}^{k,\ell} = \boldsymbol{\rho}\, \frac{\exp(-\boldsymbol{a}m\nu)\Gamma(2\mu)\, m!\, \mathcal{G}_m^{\mu}(\boldsymbol{b})}{\Gamma(2\mu+m)} f(m\nu,n)(\lambda+n)\Gamma(\lambda)\Gamma(\lambda+1)\frac{\left|\Gamma(\frac{n+\iota m\nu}{2})\right|^2}{\left|\Gamma(\lambda+1+\frac{n+\iota m\nu}{2})\right|^2}$$

Hypergeometric model 6

Covariance kernel:

$$\boldsymbol{C} = \frac{\boldsymbol{\rho}}{(1-2\boldsymbol{b}\exp(\nu(s-1-\boldsymbol{a}))r+\exp(2\nu(s-1-\boldsymbol{a})))^{\mu}} \times {}_2F_1\left(\frac{\mu}{2},\frac{\mu+1}{2};\mu+\frac{1}{2};\frac{4\exp(2\nu(s-1-\boldsymbol{a}))(1-\boldsymbol{b}^2)(1-r^2)}{(1-2\boldsymbol{b}\exp(\nu(s-1-\boldsymbol{a}))r+\exp(2\nu(s-1-\boldsymbol{a})))^2}\right)$$

Schoenberg matrices:

$$\boldsymbol{b}_{n,m}^{k,\ell} = \boldsymbol{\rho}\, \frac{\exp(-(1+\boldsymbol{a})m\nu)\Gamma(2\mu)\, m!\, \mathcal{G}_m^{\mu}(\boldsymbol{b})}{\Gamma(2\mu+m)}\, 2^{\lambda}(\lambda+n)(m\nu)^{-\lambda}\Gamma(\lambda)I_{\lambda+n}(m\nu)$$

Hypergeometric model 7

Covariance kernel:

$$\boldsymbol{C} = \frac{\boldsymbol{\rho}(1-\exp(-2\nu(\arccos(s)+\boldsymbol{a})))}{(1-2\boldsymbol{b}\exp(-\nu(\arccos(s)+\boldsymbol{a}))r+\exp(-2\nu(\arccos(s)+\boldsymbol{a})))^{\mu+1}}$$

To be continued

Table 10 (continued)

$$\times\, {}_2F_1\left(\frac{\mu+1}{2}, \frac{\mu}{2}+1; \mu+\frac{1}{2}; \frac{4\exp(-2\nu(\arccos(s)+\boldsymbol{a}))(1-\boldsymbol{b}^2)(1-r^2)}{(1-2\boldsymbol{b}\exp(-\nu(\arccos(s)+\boldsymbol{a}))r+\exp(-2\nu(\arccos(s)+\boldsymbol{a})))^2}\right)$$

Schoenberg matrices:

$$\boldsymbol{b}_{n,m}^{k,\ell} = \boldsymbol{\rho}\, \frac{\exp(-\boldsymbol{a}m\nu)\varGamma(2\mu)\, m!\,(1+\frac{m}{\mu})\,\mathcal{G}_m^{\mu}(\boldsymbol{b})}{\varGamma(2\mu+m)}\, f(m\nu,n)(\lambda+n)\varGamma(\lambda)\varGamma(\lambda+1)\frac{\left|\varGamma(\frac{n+\iota m\nu}{2})\right|^2}{\left|\varGamma(\lambda+1+\frac{n+\iota m\nu}{2})\right|^2}$$

Hypergeometric model 8

Covariance kernel:

$$\boldsymbol{C} = \frac{\boldsymbol{\rho}(1-\exp(2\nu(s-1-\boldsymbol{a})))}{(1-2\boldsymbol{b}\exp(\nu(s-1-\boldsymbol{a}))r+\exp(2\nu(s-1-\boldsymbol{a})))^{\mu+1}}$$
$$\times\, {}_2F_1\left(\frac{\mu+1}{2}, \frac{\mu}{2}+1; \mu+\frac{1}{2}; \frac{4\exp(2\nu(s-1-\boldsymbol{a}))(1-\boldsymbol{b}^2)(1-r^2)}{(1-2\boldsymbol{b}\exp(\nu(s-1-\boldsymbol{a}))r+\exp(2\nu(s-1-\boldsymbol{a})))^2}\right)$$

Schoenberg matrices:

$$\boldsymbol{b}_{n,m}^{k,\ell} = \boldsymbol{\rho}\, \frac{\exp(-(1+\boldsymbol{a})m\nu)\varGamma(2\mu)\, m!\,(1+\frac{m}{\mu})\,\mathcal{G}_m^{\mu}(\boldsymbol{b})}{\varGamma(2\mu+m)}\, 2^{\lambda}(\lambda+n)(m\nu)^{-\lambda}\varGamma(\lambda)I_{\lambda+n}(m\nu)$$

Sufficient conditions for convergence:

$\boldsymbol{a}$ with entries in $(0,\infty)$, $\boldsymbol{b} = [\langle \boldsymbol{s}_i, \boldsymbol{s}_j\rangle_\ell]_{i,j=1}^p$ for a set of points $\boldsymbol{s}_1,\ldots,\boldsymbol{s}_p \in \mathbb{S}^\ell$, $\nu > 0$ and $\boldsymbol{\rho}$ with entries in $\mathbb{R}$

Sufficient conditions for positive semidefiniteness:

(1) $\boldsymbol{a}$ is conditionally negative semidefinite
(2) $\boldsymbol{\rho}$ is positive semidefinite

Table 11: Hypergeometric covariance kernels, part 4.

Hypergeometric model 9

Covariance kernel:

$$\boldsymbol{C} = \frac{\boldsymbol{\rho}}{(1-2e^{-\nu(\arccos(s)+\boldsymbol{a})}r+e^{-2\nu(\arccos(s)+\boldsymbol{a})})^{\mu}}\exp\left(-\frac{2\boldsymbol{b}\,e^{-\nu(\arccos(s)+\boldsymbol{a})}(r-e^{-\nu(\arccos(s)+\boldsymbol{a})})}{1-2e^{-\nu(\arccos(s)+\boldsymbol{a})}r+e^{-2\nu(\arccos(s)+\boldsymbol{a})}}\right)$$
$$\times\, {}_0F_1\left(;\mu+\frac{1}{2}; \frac{e^{-2\nu(\arccos(s)+\boldsymbol{a})}\boldsymbol{b}^2(4r^2-6\,e^{-\nu(\arccos(s)+\boldsymbol{a})}r+3\,e^{-2\nu(\arccos(s)+\boldsymbol{a})}-1)}{4(1-2\,e^{-\nu(\arccos(s)+\boldsymbol{a})}r+e^{-2\nu(\arccos(s)+\boldsymbol{a})})^2}\right)$$

Schoenberg matrices:

$$\boldsymbol{b}_{n,m}^{k,\ell} = \boldsymbol{\rho}\,\exp(-\boldsymbol{a}m\nu)\,{}_1F_1(-m;2\mu;\boldsymbol{b})\,f(m\nu,n)(\lambda+n)\varGamma(\lambda)\varGamma(\lambda+1)\frac{\left|\varGamma(\frac{n+\iota m\nu}{2})\right|^2}{\left|\varGamma(\lambda+1+\frac{n+\iota m\nu}{2})\right|^2}$$

Hypergeometric model 10

To be continued

Table 11 (continued)

Covariance kernel:

$$\boldsymbol{C} = \frac{\boldsymbol{\rho}}{(1-2\exp(\nu(s-1-\boldsymbol{a}))r+\exp(2\nu(s-1-\boldsymbol{a})))^{\mu}}\exp\left(-\frac{2\boldsymbol{b}\exp(\nu(s-1-\boldsymbol{a}))(r-\exp(\nu(s-1-\boldsymbol{a})))}{1-2\exp(\nu(s-1-\boldsymbol{a}))r+\exp(2\nu(s-1-\boldsymbol{a}))}\right)$$
$$\times\, {}_0F_1\left(;\mu+\frac{1}{2};\frac{\exp(2\nu(s-1-\boldsymbol{a}))\boldsymbol{b}^2(4r^2-6\exp(\nu(s-1-\boldsymbol{a}))r+3\exp(2\nu(s-1-\boldsymbol{a}))-1)}{4(1-2\exp(\nu(s-1-\boldsymbol{a}))r+\exp(2\nu(s-1-\boldsymbol{a})))^2}\right)$$

Schoenberg matrices:

$$\boldsymbol{b}_{n,m}^{k,\ell} = \boldsymbol{\rho}\exp(-(1+\boldsymbol{a})m\nu)\,{}_1F_1(-m;2\mu;\boldsymbol{b})\,2^{\lambda}(\lambda+n)(m\nu)^{-\lambda}\Gamma(\lambda)I_{\lambda+n}(m\nu)$$

Sufficient conditions for convergence:

$\boldsymbol{a}$ with entries in $(0,\infty)$, $\nu > 0$ and $\boldsymbol{\rho}$ and $\boldsymbol{b}$ with entries in $\mathbb{R}$

Sufficient conditions for positive semidefiniteness:

(1) $\boldsymbol{a}$ is conditionally negative semidefinite
(2) $\boldsymbol{\rho}$ is positive semidefinite
(3) $-\boldsymbol{b}$ is positive semidefinite

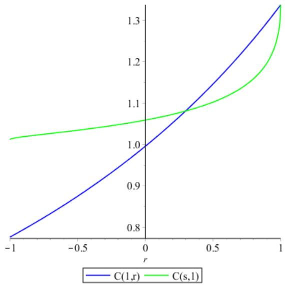

(a) Hypergeometric model 1

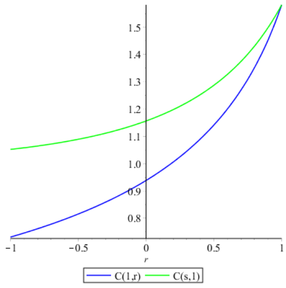

(b) Hypergeometric model 2

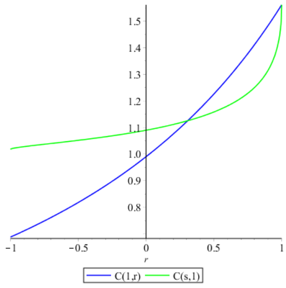

(c) Hypergeometric model 3

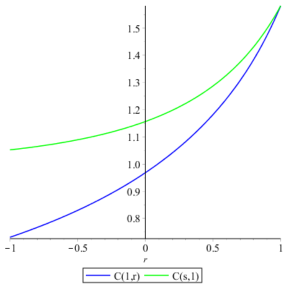

(d) Hypergeometric model 4

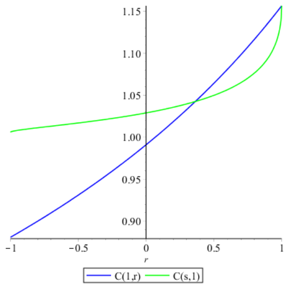

(e) Hypergeometric model 5

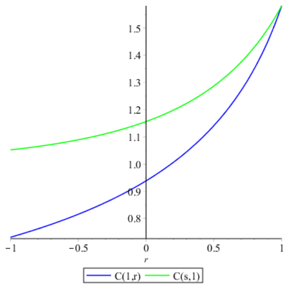

(f) Hypergeometric model 6

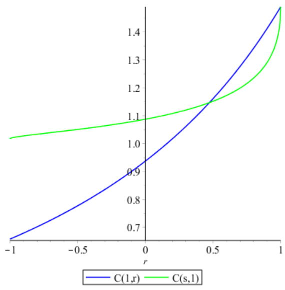

(g) Hypergeometric model 7

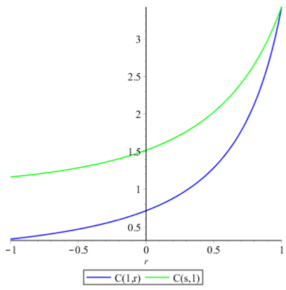

(h) Hypergeometric model 8

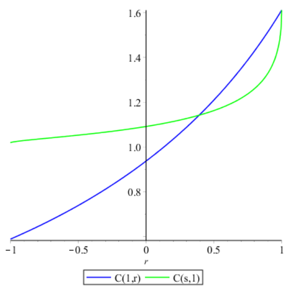

(i) Hypergeometric model 9

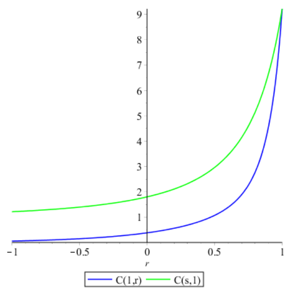

(j) Hypergeometric model 10

Fig. 3: Examples of hypergeometric models. Representation of the marginals $s \mapsto C(s,1)$ (green) and $r \mapsto C(1,r)$ (blue) for s and r ranging from -1 to 1

4 Discussion

All the covariance kernels presented in Tables 2 to 11 are nonseparable, i.e., the componentwise isotropic part $(s, r) \mapsto C(s, r)$ cannot be written as the elementwise product of a function of s with a function of r; equivalently, the Schoenberg matrix $\boldsymbol{b}_{n,m}^{k,\ell}$ cannot be written as the elementwise product of a matrix depending on n with a matrix depending on m. This is illustrated in Figure 4, which shows the full covariance maps (not only the marginals) for two specific models of the above list: in both cases, the curvature of the isopleths is not compatible with a separable covariance. The interest in nonseparable covariance kernels for random fields defined on $\mathbb{S}^k \times \mathbb{S}^\ell$ lies in the fact that they allow modeling complex interactions between the spatial variations on $\mathbb{S}^k$ and that on $\mathbb{S}^\ell$. To date, many nonseparable covariance kernels have been designed for modeling data indexed in a Euclidean space (Cressie and Huang, 1999; Gneiting, 2002; Stein, 2005; Apanasovich and Genton, 2010; Rodrigues and Diggle, 2010; Allard et al., 2022) or the product of a Euclidean space with a sphere (Shirota and Gelfand, 2017; Porcu et al., 2016; Alegría et al., 2019; Emery et al., 2021), but we are not aware of such kernels for modeling data indexed in the product of two spheres, except for the recent works of Bachoc et al. (2021) and Porcu and White (2022).

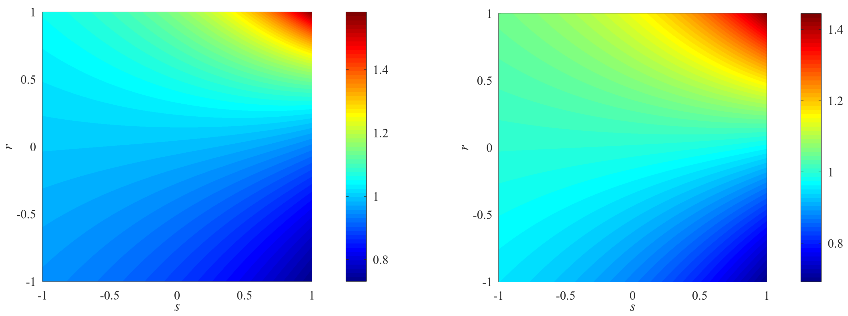

(a) Elementary model 1 with $\mu = 1/2$, $a = 2$, $b = 0$, $\nu = 1$ and $\rho = 1$

(b) Bessel model 1 with $\mu = 1/2$, $a = 2$, $b = 0$, $\nu = 1$ and $\rho = 1$

Fig. 4: Mapping $(s, r) \mapsto C(s, r)$ for s and r ranging from -1 to 1, for the elementary model 1 and Bessel model 1 whose marginals are shown in Figures 1 and 2, respectively

The expression of the proposed kernels contain up to five matrix-valued parameters, which are often necessary to ensure the convergence of the Schoenberg sequence, i.e., the existence of the kernel. As an exception, in Tables 2, 4 and 6, either the matrix-valued parameter $\boldsymbol{a}$ or the matrix-valued parameter $\boldsymbol{b}$ can be set to zero, but not both simultaneously, while $\boldsymbol{b}$ can also be set to zero to yield more parsimonious kernels in Table 11. However, all these are minor simplifications, and dealing with 3 to 5 parameters allows an interesting trade-off between the number of parameters and the structural features that can be fitted. In particular, from the previous figures, one sees that the behavior at short distances (s or r close to 1), shape and monotonicity of the marginal covariances can be different. The same happens with multivariate kernels: the parameters controlling the shape, large-scale and short-scale behaviors can be different for all the entries of the covariance, which offers much more versatility to the practitioners than traditional modeling approaches such as the well-known and parameter-intensive linear model of coregionalization (Chilès and Delfiner, 2012; Genton and Kleiber, 2015). In our constructions, the conditions on the matrix-valued parameters refer to positive semidefiniteness and negative conditional semidefiniteness and are straightforward to check (see criteria in Section 2.1).

The case of the hypertorus $\mathbb{T}^{1,\ell}$ deserves a separate treatment. Tables 2 to 11 provide covariance kernels on $\mathbb{T}^{k,\ell} \times \mathbb{T}^{k,\ell}$ together with their (k,ℓ)-Schoenberg sequences, for any integers k and ℓ greater than 1. In particular, the following holds:

(1) Each (k,ℓ)-Schoenberg matrix $\boldsymbol{b}_{n,m}^{k,\ell}$ is positive semidefinite.
(2) The series $\sum_{n=0}^{\infty}\sum_{m=0}^{\infty} \boldsymbol{b}_{n,m}^{k,\ell} \mathcal{G}_n^{(k-1)/2}(s)\mathcal{G}_m^{(\ell-1)/2}(r)$ converges (pointwise and componentwise) to $\boldsymbol{C}(s,r)$ for any $s,r \in [-1,1]$.
(3) For all the presented models, the analytical expression of $\boldsymbol{C}$ depends on ℓ (equivalently, μ) but not on k (equivalently, λ).

Looking at the proofs in Appendix A and in Emery et al. (2022), it is seen that the positive semidefiniteness of the Schoenberg matrices (1) and the convergence of the Schoenberg series (2) actually hold for any real numbers (not necessarily integers) k and ℓ greater than 1. If one makes k tend to 1, with $\ell > 1$ fixed, it becomes possible to extend the previous kernels to the hypertorus $\mathbb{T}^{1,\ell}$, which is of interest for modeling variables evolving in time or direction-dependent variables (recall Section 1).

Specifically, for each fixed natural integer m, define

$$\boldsymbol{b}_{n,m}^{1,\ell} = \begin{cases} \lim_{k\to 1} \boldsymbol{b}_{n,m}^{k,\ell} \text{ if } n = 0 \\ \lim_{k\to 1} \frac{2\lambda}{n}\boldsymbol{b}_{n,m}^{k,\ell} \text{ if } n > 0. \end{cases}$$

The above limits exist and are finite for all the models of Tables 2 to 11, insofar as the Schoenberg matrix always contains a term $\Gamma(\lambda)(\lambda+n)$, with $\lambda = \frac{k-1}{2}$ and

$$\begin{cases} \lim_{\lambda\to 0} \Gamma(\lambda)(\lambda+n) = 1 \text{ if } n = 0 \\ \lim_{\lambda\to 0} \frac{2\lambda}{n}\Gamma(\lambda)(\lambda+n) = 2 \text{ if } n > 0. \end{cases}$$

Also, $\boldsymbol{b}_{n,m}^{1,\ell}$ is the limit of a sequence of positive semidefinite matrices, hence it is positive semidefinite for any n and m. Accordingly, taking the limit of both sides of (5) as k tends to 1, one obtains:

$$\begin{aligned}\lim_{k\to 1} \boldsymbol{C}(s,r) &= \lim_{k\to 1} \sum_{n=0}^{\infty}\sum_{m=0}^{\infty} \boldsymbol{b}_{n,m}^{k,\ell} \mathcal{G}_n^{(k-1)/2}(s)\mathcal{G}_m^{(\ell-1)/2}(r)\\ &= \lim_{k\to 1} \sum_{m=0}^{\infty} \boldsymbol{b}_{0,m}^{k,\ell} \mathcal{G}_0^{(k-1)/2}(s)\mathcal{G}_m^{(\ell-1)/2}(r)\\ &+ \lim_{k\to 1} \sum_{n=1}^{\infty}\sum_{m=0}^{\infty} \frac{2\lambda}{n}\boldsymbol{b}_{n,m}^{k,\ell} \frac{n}{2\lambda}\mathcal{G}_n^{(k-1)/2}(s)\mathcal{G}_m^{(\ell-1)/2}(r), \quad s,r\in[-1,1],\end{aligned}$$

i.e.,

$$\boldsymbol{C}(s,r) = \sum_{n=0}^{\infty}\sum_{m=0}^{\infty} \boldsymbol{b}_{n,m}^{1,\ell} \mathcal{G}_n^{0}(s)\mathcal{G}_m^{(\ell-1)/2}(r), \quad s,r\in[-1,1], \tag{7}$$

where $\mathcal{G}_n^0$ is the Chebyshev polynomial of the first kind (Olver et al., 2010, formula 18.7.25):

$$\mathcal{G}_n^0 = \begin{cases} 1 \text{ if } n=0 \\ \lim_{\lambda\to 0} \frac{n}{2\lambda}\mathcal{G}_n^\lambda \text{ if } n>0. \end{cases}$$

The identity (7) gives a valid $(1,\ell)$-Schoenberg sequence for the mapping $\boldsymbol{C}$, viewed as the componentwise isotropic part of a covariance on the hypertorus $\mathbb{T}^{1,\ell}$.

Finally, a side product of this work is the design of new p-variate isotropic covariance kernels on spheres or hyperspheres, together with sufficient validity conditions on their parameters. Indeed, for all the models presented in Tables 2 to 11, the marginals $s\mapsto \boldsymbol{C}(s,1)$ and $r\mapsto \boldsymbol{C}(1,r)$ belong to $\mathcal{P}^p(\mathbb{S}^k)$ and $\mathcal{P}^p(\mathbb{S}^\ell)$, respectively. The marginals obtained by setting s to 1 have already been studied in Emery et al. (2022). Likewise, the marginals obtained by setting r to 1 are members of $\mathcal{P}^p(\mathbb{S}^k)$ and their spectral representation is derived from (5):

$$\boldsymbol{C}(s,1) = \sum_{n=0}^{\infty} \boldsymbol{b}_n^k\, \mathcal{G}_n^{(k-1)/2}(s), \quad s\in[-1,1],$$

with

$$\boldsymbol{b}_n^k = \sum_{m=0}^{\infty} \boldsymbol{b}_{n,m}^{k,\ell}\, \mathcal{G}_m^{(\ell-1)/2}(1), \quad n\in\mathbb{N}.$$

5 Estimation and simulation

A common challenge in spatial statistics is the estimation of the covariance parameters from a set of sampling data (observations). Having chosen a parametric class of covariance models among those presented in Tables 2 to 11 and assuming that the random field under study is Gaussian, maximum likelihood techniques can be used to specify the model parameters. In the presence of large datasets, composite or pairwise likelihood may be good alternatives to full likelihood (Curriero and Lele, 1999; Varin and Vidoni, 2005). Also, the maximization of the likelihood function can be done with iterative optimization algorithms that work sequentially on a subset of parameters and leave the other parameters fixed to the values previously attained; the reader is referred to Bourotte et al. (2016) and Allard et al. (2022) for details on the procedure and convincing examples. Although it has been developed for modeling data in Euclidean spaces, this procedure can be adapted to data on hypertori and benefits from the fact that all the kernels presented in this work are relatively parsimonious (with two to five matrix-valued parameters), so as to reach a trade-off between model complexity, interpretability and versatility and to avoid overfitting.

We now turn into the simulation of Gaussian vector random fields that are continuously indexed over the hypertorus.

For each model in Tables 2 to 11, the Schoenberg sequence has a known analytic expression, which makes possible to simulate a Gaussian vector random field on the hypertorus by spectral algorithms. A straightforward extension of the arguments exposed in Alegría et al. (2020) implies that a zero-mean vector random field $\boldsymbol{Z}$ on $\mathbb{T}^{k,\ell}$ with matrix-valued covariance $\boldsymbol{K}$ associated with the Schoenberg sequence $\{\boldsymbol{b}_{n,m}^{k,\ell}\}_{n,m=0}^{\infty}$ can be obtained by putting

$$\boldsymbol{Z}(\mathbf{x}) = \varepsilon \sqrt{\frac{p(2\kappa_1 + k - 1)(2\kappa_2 + \ell - 1)}{a_{\kappa_1,\kappa_2}(k-1)(\ell-1)}}\, \boldsymbol{\gamma}_{\kappa_1,\kappa_2,k,\ell}^{(q)}\, \mathcal{G}_{\kappa_1}^{(k-1)/2}(\langle \omega_1, x\rangle_k)\, \mathcal{G}_{\kappa_2}^{(\ell-1)/2}(\langle \omega_2, y\rangle_\ell), \tag{8}$$

where:

(1) $\mathbf{x} = (x, y) \in \mathbb{T}^{k,\ell} = \mathbb{S}^k \times \mathbb{S}^\ell$, with $k, \ell > 1$
(2) ε is a random variable with a Rademacher distribution (symmetric two-point distribution concentrated at 1 and +1)
(3) $\boldsymbol{\kappa} = (\kappa_1, \kappa_2)$, where κ_1 and κ_2 are random integers with joint probability mass $\mathbb{P}(\kappa_1 = n, \kappa_2 = m) = a_{n,m}$ for any nonnegative integers n and m
(4) $a_{n,m} > 0$ for any (n, m) such that $\boldsymbol{b}_{n,m}^{k,\ell}$ is nonzero
(5) q is a random integer uniformly distributed in $\{1, \ldots, p\}$
(6) $\boldsymbol{\gamma}_{n,m,k,\ell}$ is the positive semidefinite square root of $\boldsymbol{b}_{n,m}^{k,\ell}$
(7) $\boldsymbol{\gamma}_{n,m,k,\ell}^{(q)}$ is the q-th column of $\boldsymbol{\gamma}_{n,m,k,\ell}$
(8) ω_1 and ω_2 are random vectors uniformly distributed on $\mathbb{S}^k$ and $\mathbb{S}^\ell$, respectively
(9) ε, $\boldsymbol{\kappa}$, q, ω_1 and ω_2 are mutually independent.

Other constructions are possible, e.g., by using hyperspherical harmonics instead of Gegenbauer polynomials in (8) (Emery and Porcu, 2019).

For $k = 1$ and $\ell > 1$, the simulated random field takes the form

$$\boldsymbol{Z}(\mathbf{x}) = \varepsilon \sqrt{\frac{2p(2\kappa_2 + \ell - 1)}{a_{\kappa_1,\kappa_2}(\ell - 1)}} \boldsymbol{\gamma}^{(q)}_{\kappa_1,\kappa_2,1,\ell} \, \mathcal{G}^0_{\kappa_1}(\langle \omega_1, x \rangle_k) \, \mathcal{G}^{(\ell-1)/2}_{\kappa_2}(\langle \omega_2, y \rangle_\ell), \quad \mathbf{x} = (x, y) \in \mathbb{T}^{1,\ell}. \tag{9}$$

Finally, a zero-mean Gaussian random field with covariance $\boldsymbol{K}$ can be obtained via a central limit approximation of the form

$$\widetilde{\boldsymbol{Z}}(\mathbf{x}) = \frac{1}{\sqrt{J}} \sum_{j=1}^{J} \boldsymbol{Z}_j(\mathbf{x}), \quad \mathbf{x} \in \mathbb{T}^{k,\ell}, \tag{10}$$

where J is a large integer and $\{\boldsymbol{Z}_j : j = 1, \ldots, J\}$ is a set of independent copies of $\boldsymbol{Z}$ as defined in (8) (if $k > 1$) or (9) (if $k = 1$).

Although any bivariate probability mass function such that $a_{n,m} > 0$ if $\boldsymbol{b}^{k,\ell}_{n,m} \neq \mathbf{0}$ is acceptable for simulating the random degrees (κ_1, κ_2), some choices are more judicious than others to improve the central limit approximation. In particular, if $\boldsymbol{b}^{k,\ell}_{n,m} = \mathbf{0}$, then $\boldsymbol{\gamma}_{n,m,k,\ell} = \mathbf{0}$ and the pair (n, m) contributes with a zero (constant) field to the sum (8) or (9). Accordingly, it is good practice to choose $a_{n,m} = 0$ when $\boldsymbol{b}^{k,\ell}_{n,m} = \mathbf{0}$, in order not to use a copy of $\boldsymbol{Z}$ that does not add any spatial variability. Also, for the sake of simplicity, it is suggested that κ_1 and κ_2 are independent. Based on these arguments, a good choice for $a_{n,m}$ is the product of two long-tailed probability mass functions, for instance (shifted zeta distributions of parameter 2)

$$a_{n,m} = \frac{36}{\pi^4}(1 + n)^{-2}(1 + m)^{-2}, \quad n, m \in \mathbb{N}.$$

This choice is certainly not the best option for the elementary models 4, 5, 9 and 10, for which $\boldsymbol{b}^{k,\ell}_{n,m} = \mathbf{0}$ for $m > \kappa$. In such cases, one suggestion is the product of a shifted zeta distribution with a uniform distribution:

$$a_{n,m} = \begin{cases} \frac{6}{(1+\kappa)\pi^2}(1 + n)^{-2}, & n \in \mathbb{N} \text{ and } m \leq \kappa \\ 0, & n \in \mathbb{N} \text{ and } m > \kappa. \end{cases}$$

The computational cost for constructing a realization of $\widetilde{\boldsymbol{Z}}$ as in (10) is essentially proportional to the number of copies J and to the number of target locations on the hypertorus, while the memory requirements are minimal (the simulated values can be exported as soon as they are generated). The calculations are furthermore parallelizable, which makes the proposed spectral algorithm an attractive approach when large-scale simulations are required.

6 Concluding remarks

The present paper has provided a rich catalogue of matrix-valued covariance kernels, together with their spectral representations and sufficient validity conditions on the parameters, for vector random fields indexed over hypertori. This catalogue may be useful for practitioners who deal with the modeling of direction-dependent (e.g., electromagnetic radiation, temperature gradient, gravity gradient, topographic slope, tectonic plate motion, wind speed, ocean current velocity) or seasonal-dependent (e.g., temperature, precipitation, humidity, pressure, air quality, solar radiation) variables observed over a large portion of planet Earth. The paper has also provided a straightforward simulation algorithm for random fields on hypertori, for which the knowledge of the spectral representation of the covariance kernel is relevant.

Understanding the regularity properties of random fields is a subject of major importance in probability theory and statistics, for which an abundant literature is available. The works by Lang and Schwab (2015), Clarke et al. (2018) and Cleanthous et al. (2021) suggest that extensions of the mentioned approaches to our models might be doable. This is certainly a subject of interest for future researches.

Acknowledgements This work was supported by the National Agency for Research and Development of Chile [grants ANID/FONDECYT/REGULAR/No. 1210050 and ANID PIA AFB220002] and FAPESP, Brazil [grant 2021/04269-0].

Conflict of interest

The authors declare that they have no conflict of interest.

Declarations

Funding. The first author acknowledges funding of the National Agency for Research and Development of Chile, through grants ANID / FONDECYT / REGULAR / 1210050 and ANID PIA AFB220002. The second author acknowledges funding of FAPESP, grant # 2021/04269-0, Brazil. Emilio Porcu is supported by FSU-2021-016 from Khalifa University of Science and Technology.

Availability of data and material. Not applicable.

Code availability. Not applicable.

Ethics approval. Not applicable.

Consent to participate. Not applicable.

Consent for publication. Not applicable.

A Appendix: Proofs for the models in Tables 2 to 11

Lemma 1 *Let k be a positive integer and $\lambda = \frac{k-1}{2}$. Let $\{\boldsymbol{b}_n\}_{n=0}^{\infty}$ be a sequence of symmetric positive semidefinite matrices, such that the series $\sum_{n=0}^{\infty} \boldsymbol{b}_n \mathcal{G}_n^{\lambda}(s)$ converges elementwise for all $s \in [-1,1]$. Then, the series is not only convergent, but also absolutely convergent.*

Proof For $n \in \mathbb{N}$, let $\boldsymbol{b}_n = [b_{ij,n}]_{i,j=1}^{p}$. The diagonal entries $b_{ii,n}$, $i = 1,\ldots,p$, are nonnegative, while the absolute value of the off-diagonal entries can be upper bounded by use of Cauchy-Schwarz's and AM-GM inequalities:

$$|b_{ij,n}| \leq \sqrt{b_{ii,n}\, b_{jj,n}} \leq \frac{b_{ii,n} + b_{jj,n}}{2}.$$

Accordingly, the absolute convergence of the series $\sum_{n=0}^{\infty} \boldsymbol{b}_n \mathcal{G}_n^{\lambda}(s)$ stems from the fact that, for any $s \in [-1,1]$, $|\mathcal{G}_n^{\lambda}(s)| \leq \mathcal{G}_n^{\lambda}(1)$ (Olver et al., 2010, formula 18.14.4):

$$\sum_{n=0}^{\infty} |b_{ij,n} \mathcal{G}_n^{\lambda}(s)| \leq \frac{1}{2}\left(\sum_{n=0}^{\infty} b_{ii,n} \mathcal{G}_n^{\lambda}(1) + \sum_{n=0}^{\infty} b_{jj,n} \mathcal{G}_n^{\lambda}(1)\right) < \infty, \quad s \in [-1,1], i,j = 1,\ldots,p.$$

Lemma 2 *Let k, ℓ be positive integers, $\lambda = \frac{k-1}{2}$ and $\mu = \frac{\ell-1}{2}$. Also, let $\{\boldsymbol{b}_{n,m}^{k,\ell}\}_{n,m=0}^{\infty}$ be a doubly-indexed sequence of symmetric positive semidefinite matrices such that the double series $\sum_{m=0}^{\infty} \sum_{n=0}^{\infty} \boldsymbol{b}_{n,m}^{k,\ell} \mathcal{G}_n^{\lambda}(s) \mathcal{G}_m^{\mu}(r)$ converges elementwise for all $s, r \in [-1,1]$. Then, this series is absolutely convergent and one can interchange the order of the summations:*

$$-\infty < \sum_{m=0}^{\infty} \sum_{n=0}^{\infty} \boldsymbol{b}_{n,m}^{k,\ell} \mathcal{G}_n^{\lambda}(s) \mathcal{G}_m^{\mu}(r) = \sum_{n=0}^{\infty} \sum_{m=0}^{\infty} \boldsymbol{b}_{n,m}^{k,\ell} \mathcal{G}_m^{\mu}(r) \mathcal{G}_n^{\lambda}(s) < \infty, \quad s, r \in [-1,1].$$

Proof The absolute convergence can be established in the same way as in Lemma 1. The interchange of the summation order follows from Fubini's theorem for the counting measure on $\mathbb{N}$.

We can now prove the results given in Tables 2 to 11.

Let k and ℓ be integers greater than 1, $\lambda = \frac{k-1}{2}$ and $\mu = \frac{\ell-1}{2}$. Let $\boldsymbol{C}_0(\cdot\,; \boldsymbol{\alpha}, \boldsymbol{\theta})$ be the isotropic part of a continuous p-variate covariance kernel on $\mathbb{S}^{\ell}$, i.e., $\boldsymbol{C}_0 \in \mathcal{P}^p(\mathbb{S}^{\ell})$, where $\boldsymbol{\alpha}$ and $\boldsymbol{\theta}$ are real matrices of parameters, the former with size $p \times p$ and entries in $(\alpha_{\min}, \alpha_{\max})$ such that $\alpha_{\max} > 0 \geq \alpha_{\min}$. Assume that $\boldsymbol{C}_0$ has a spectral representation of the form

$$\boldsymbol{C}_0(r; \boldsymbol{\alpha}, \boldsymbol{\theta}) = \sum_{m=0}^{\infty} \boldsymbol{\alpha}^{\phi_m}\, \boldsymbol{\theta}_m\, \mathcal{G}_m^{\mu}(r), \quad r \in [-1,1], \tag{11}$$

where ϕ_m and $\boldsymbol{\theta}_m$ are a nonnegative integer and a $p \times p$ matrix, respectively, that depend analytically on $\boldsymbol{\theta}$ and m, but not on $\boldsymbol{\alpha}$.

Let now $\boldsymbol{C}_1(\cdot\,; \boldsymbol{\beta})$ be the isotropic part of a continuous p-variate covariance kernel on $\mathbb{S}^k$, i.e., $\boldsymbol{C}_1 \in \mathcal{P}^p(\mathbb{S}^k)$, where $\boldsymbol{\beta}$ is a real matrix of parameters, such that, for any nonnegative integer m, the k-Schoenberg sequence of $[\boldsymbol{C}_1]^{\phi_m}$ has a known analytical expression:

$$[\boldsymbol{C}_1(s; \boldsymbol{\beta})]^{\phi_m} = \sum_{n=0}^{\infty} \boldsymbol{\beta}_{n,\phi_m}\, \mathcal{G}_n^{\lambda}(s), \quad s \in [-1,1]. \tag{12}$$

The series (12) converges elementwise for any $s \in [-1, 1]$ and $m \in \mathbb{N}$, insofar as $[\boldsymbol{C}_1]^{\phi_m} \in \mathcal{P}^p(\mathbb{S}^k)$ for any $m \in \mathbb{N}$.

For $n, m \in \mathbb{N}$, define the matrix

$$\boldsymbol{b}_{n,m}^{k,\ell} = \boldsymbol{\beta}_{n,\phi_m}\,\boldsymbol{\theta}_m. \tag{13}$$

Based on the previous statements and on Lemma 2, if the entries of $\boldsymbol{C}_1$ take values in the open interval $(\alpha_{\min}, \alpha_{\max})$ and $\boldsymbol{b}_{n,m}^{k,\ell}$ is positive semidefinite for any $n, m \in \mathbb{N}$, the composite function $(s, r) \mapsto \boldsymbol{C}(s, r) := \boldsymbol{C}_0(r; \boldsymbol{C}_1(s; \boldsymbol{\beta}), \boldsymbol{\theta})$ defined on $[-1, 1]^2$ has a representation of the form (5) and belongs to $\mathcal{P}^p(\mathbb{T}^{k,\ell})$.

Tables 12 and 13 indicate the functions $\boldsymbol{C}_0$ and $\boldsymbol{C}_1$ used to construct the 26 kernels presented in Tables 2 to 11, and give the analytical expressions of ϕ_m, $\boldsymbol{\theta}_m$ and $\boldsymbol{\beta}_{n,m}$ as defined in (11) and (12). We refer the reader to Emery et al. (2022) for a derivation of such expressions and for a proof that $\boldsymbol{C}_0$ and $\boldsymbol{C}_1$ belong to $\mathcal{P}^p(\mathbb{S}^\ell)$ and $\mathcal{P}^p(\mathbb{S}^k)$, respectively. From this information, it is straightforward to derive the analytical expressions of the kernels and of their Schoenberg sequences (as per (13)) given in Tables 2 to 11.

Convergence of the Schoenberg sequence (5) *of* $\boldsymbol{C}$. $(\alpha_{\min}, \alpha_{\max}) = (-1, 1)$ for all the entries of Table 12, except for the one associated with the hypergeometric kernels 1 and 2, in which case $(\alpha_{\min}, \alpha_{\max}) = (-\sqrt{2}/2, \sqrt{2}/2)$. The fact that the entries of $\boldsymbol{C}_1$ take values in the open interval $(\alpha_{\min}, \alpha_{\max})$ can easily be verified on the basis of the convergence conditions given in Tables 2 to 11.

Positive semidefiniteness of the Schoenberg matrix $\boldsymbol{b}_{n,m}^{k,\ell}$. Based on the criteria given in Section 2.1 and on the positive semidefiniteness conditions given in Emery et al. (2022), the conditions indicated in Tables 2 to 11 ensure that $\boldsymbol{\theta}_m$ and $\boldsymbol{\beta}_{n,m}$ are positive semidefinite matrices for any nonnegative integers m and n. The positive semidefiniteness of the Schoenberg matrix (13) follows from the Schur product theorem, which concludes the proof.

References

Alegría, A., Emery, X., and Lantuéjoul, C. (2020). The turning arcs: a computationally efficient algorithm to simulate isotropic vector-valued Gaussian random fields on the d-sphere. *Statistics and Computing*, 30(5):1403–1418.

Alegría, A., Porcu, E., Furrer, R., and Mateu, J. (2019). Covariance functions for multivariate Gaussian fields evolving temporally over planet earth. *Stochastic Environmental Research and Risk Assessment*, 33(8):1593–1608.

Allard, D., Clarotto, L., and Emery, X. (2022). Fully nonseparable Gneiting covariance functions for multivariate space-time data. *Spatial Statistics*, 52:100706.

Apanasovich, T. V. and Genton, M. G. (2010). Cross-covariance functions for multivariate random fields based on latent dimensions. *Biometrika*, 97:15 –30.

Aronszajn, N. (1950). Theory of reproducing kernels. *Transactions of the American Mathematical Society*, 68(3):337–404.

Bachoc, F., Peron, A. P., and Porcu, E. (2021). Multivariate Gaussian random fields over generalized product spaces involving the hypertorus. *Theory of Probability and Mathematical Statistics*, in press.

Berg, C., Christensen, J. P. R., and Ressel, P. (1984). *Harmonic analysis on semigroups*, volume 100 of *Graduate Texts in Mathematics*. Springer-Verlag, New York.

Bevilacqua, M., Diggle, P. J., and Porcu, E. (2020). Families of covariance functions for bivariate random fields on spheres. *Spatial Statistics*, 40:100448.

Bonfim, R. N. and Menegatto, V. A. (2016). Strict positive definiteness of multivariate covariance functions on compact two-point homogeneous spaces. *Journal of Multivariate Analysis*, 152:237–248.

Bourotte, M., Allard, D., and Porcu, E. (2016). A flexible class of non-separable cross-covariance functions for multivariate space–time data. *Spatial Statistics*, 18:125–146.

Table 12: List of functions $\boldsymbol{C}_0$ and associated parameters used to construct the covariance kernels given in Tables 2 to 11

Kernel	$\boldsymbol{C}_0(r;\boldsymbol{\alpha},\boldsymbol{\theta})$	ϕ_m	$\boldsymbol{\theta}_m$
Elementary 1 & 6	$\boldsymbol{\rho}\,(1-2\boldsymbol{\alpha}r+\boldsymbol{\alpha}^2)^{-\mu}$	m	$\boldsymbol{\rho}$
Elementary 2 & 7	$\boldsymbol{\rho}\,(1-\boldsymbol{\alpha}r)(1-2\boldsymbol{\alpha}r+\boldsymbol{\alpha}^2)^{-\mu-1}$	m	$\boldsymbol{\rho}\frac{(m+2\mu)}{4\mu}$
Elementary 3 & 8	$\boldsymbol{\rho}\,2^{\mu-\frac{1}{2}}(1-2\boldsymbol{\alpha}r+\boldsymbol{\alpha}^2)^{-\frac{1}{2}}(1-\boldsymbol{\alpha}r+\sqrt{1-2\boldsymbol{\alpha}r+\boldsymbol{\alpha}^2})^{\frac{1}{2}-\mu}$	m	$\frac{\boldsymbol{\rho}\,(\mu+\frac{1}{2})_m}{(2\mu)_m}$
Elementary 4 & 9	$\boldsymbol{\rho}\,(1+2\boldsymbol{\alpha}\,r+\boldsymbol{\alpha}^2)^{\frac{\kappa}{2}}\,\mathcal{G}_\kappa^\mu\left(\frac{r+\boldsymbol{\alpha}}{\sqrt{1+2\boldsymbol{\alpha}\,r+\boldsymbol{\alpha}^2}}\right)$	$\kappa-m$	$\begin{cases}\mathbf{0} & \text{if } m>\kappa\\ \boldsymbol{\rho}\,\frac{\Gamma(\kappa+2\mu)}{(\kappa-m)!\,\Gamma(m+2\mu)} & \text{otherwise}\end{cases}$
Elementary 5 & 10	$\boldsymbol{\rho}\,(1+2\boldsymbol{\alpha}\,r+\boldsymbol{\alpha}^2)^{\frac{\kappa}{2}}\,\mathcal{G}_\kappa^\mu\left(\frac{1+\boldsymbol{\alpha}\,r}{\sqrt{1+2\boldsymbol{\alpha}\,r+\boldsymbol{\alpha}^2}}\right)$	m	$\begin{cases}\mathbf{0} & \text{if } m>\kappa\\ \boldsymbol{\rho}\,\frac{\Gamma(\kappa+2\mu)}{(\kappa-m)!\,\Gamma(m+2\mu)} & \text{otherwise}\end{cases}$
Special 1 & 2	$\boldsymbol{\rho}\frac{\Gamma(2\mu)\,\Gamma(\boldsymbol{\kappa}+1)}{\Gamma(\boldsymbol{\kappa}+2\mu)\,(1-2\boldsymbol{\alpha}r+\boldsymbol{\alpha}^2)^{\mu+\boldsymbol{\kappa}/2}}\,\mathcal{G}_{\boldsymbol{\kappa}}^\mu\left(\frac{1-\boldsymbol{\alpha}r}{\sqrt{1-2\boldsymbol{\alpha}r+\boldsymbol{\alpha}^2}}\right)$	m	$\boldsymbol{\rho}\frac{(\boldsymbol{\kappa}+2\mu)_m}{(2\mu)_m}$
Bessel 1 & 3	$\boldsymbol{\rho}\Gamma(\mu+\frac{1}{2})\,\exp(\boldsymbol{\alpha}\,r)\left(\frac{1}{2}\,\boldsymbol{\alpha}\,(1-r^2)^{1/2}\right)^{\frac{1}{2}-\mu}J_{\mu-\frac{1}{2}}(\boldsymbol{\alpha}\,(1-r^2)^{1/2})$	m	$\frac{\boldsymbol{\rho}}{(2\mu)_m}$
Bessel 2 & 4	$\boldsymbol{\rho}\left(\frac{1}{2}\boldsymbol{\alpha}(1-r^2)^{1/2}\right)^{\frac{1}{2}-\mu}J_{\mu-\frac{1}{2}}(\sqrt{2\boldsymbol{\alpha}(1-r)})\,I_{\mu-\frac{1}{2}}(\sqrt{2\boldsymbol{\alpha}(1+r)})$	m	$\frac{\boldsymbol{\rho}}{\Gamma(\mu+\frac{1}{2})\,\Gamma(\mu+m+\frac{1}{2})\,(2\mu)_m}$
Hypergeometric 1 & 2	$\frac{\boldsymbol{\rho}}{(1-\boldsymbol{\alpha}r)^{\boldsymbol{\kappa}}}\,{}_2F_1\left(\frac{\boldsymbol{\kappa}}{2},\frac{\boldsymbol{\kappa}+1}{2};\mu+\frac{1}{2};-\frac{\boldsymbol{\alpha}^2\,(1-r^2)}{(1-\boldsymbol{\alpha}r)^2}\right)$	m	$\boldsymbol{\rho}\frac{(\boldsymbol{\kappa})_m}{(2\mu)_m}$
Hypergeometric 3 & 4	$\boldsymbol{\rho}\,{}_2F_1\left(\boldsymbol{\kappa},2\mu-\boldsymbol{\kappa};\mu+\frac{1}{2};\frac{1-\boldsymbol{\alpha}-\sqrt{1-2\boldsymbol{\alpha}r+\boldsymbol{\alpha}^2}}{2}\right)$ $\times\,{}_2F_1\left(\boldsymbol{\kappa},2\mu-\boldsymbol{\kappa};\mu+\frac{1}{2};\frac{1+\boldsymbol{\alpha}-\sqrt{1-2\boldsymbol{\alpha}r+\boldsymbol{\alpha}^2}}{2}\right)$	m	$\boldsymbol{\rho}\,\frac{(2\mu-\boldsymbol{\kappa})_n\,(\boldsymbol{\kappa})_m}{(2\mu)_m\,(\mu+\frac{1}{2})_m}$
Hypergeometric 5 & 6	$\frac{\boldsymbol{\rho}}{(1-2\boldsymbol{\alpha}\boldsymbol{b}r+\boldsymbol{\alpha}^2)^\mu}\,{}_2F_1\left(\frac{\mu}{2},\frac{\mu+1}{2};\mu+\frac{1}{2};\frac{4\boldsymbol{\alpha}^2(1-\boldsymbol{b}^2)(1-r^2)}{(1-2\boldsymbol{\alpha}\boldsymbol{b}r+\boldsymbol{\alpha}^2)^2}\right)$	m	$\boldsymbol{\rho}\frac{\Gamma(2\mu)\,m!}{\Gamma(2\mu+m)}\,\mathcal{G}_m^\mu(\boldsymbol{b})$
Hypergeometric 7 & 8	$\frac{\boldsymbol{\rho}\,(1-\boldsymbol{\alpha}^2)}{(1-2\boldsymbol{\alpha}\boldsymbol{b}r+\boldsymbol{\alpha}^2)^{\mu+1}}\,{}_2F_1\left(\frac{\mu+1}{2},\frac{\mu}{2}+1;\mu+\frac{1}{2};\frac{4\boldsymbol{\alpha}^2(1-\boldsymbol{b}^2)(1-r^2)}{(1-2\boldsymbol{\alpha}\boldsymbol{b}r+\boldsymbol{\alpha}^2)^2}\right)$	m	$\boldsymbol{\rho}\frac{\Gamma(2\mu)\,m!}{\Gamma(2\mu+m)}\left(1+\frac{m}{\mu}\right)\mathcal{G}_m^\mu(\boldsymbol{b})$
Hypergeometric 9 & 10	$\frac{\boldsymbol{\rho}}{(1-2\boldsymbol{\alpha}r+\boldsymbol{\alpha}^2)^\mu}\,\exp\left(-\frac{2\boldsymbol{\alpha}\boldsymbol{b}(r-\boldsymbol{\alpha})}{1-2\boldsymbol{\alpha}r+\boldsymbol{\alpha}^2}\right)$ $\times\,{}_0F_1\left(;\mu+\frac{1}{2};\frac{\boldsymbol{\alpha}^2\,\boldsymbol{b}^2\,(4r^2-6\boldsymbol{\alpha}r+3\boldsymbol{\alpha}^2-1)}{4(1-2\boldsymbol{\alpha}r+\boldsymbol{\alpha}^2)^2}\right)$	m	$\boldsymbol{\rho}\,{}_1F_1\,(-m;2\mu;\boldsymbol{b})$

Table 13: List of functions $\boldsymbol{C}_1$ and associated parameters used to construct the covariance kernels given in Tables 2 to 11

Kernel	$\boldsymbol{C}_1(s;\boldsymbol{\beta})$	$\boldsymbol{\beta}_{n,m}$
Elementary 1 to 5, Bessel 1 & 2	$\exp(-\boldsymbol{\nu}\boldsymbol{a}-\boldsymbol{b})\exp(\boldsymbol{\nu}s)$	$\exp(-m\boldsymbol{\nu}\boldsymbol{a}-m\boldsymbol{b})2^\lambda\Gamma(\lambda)(\lambda+n)(m\boldsymbol{\nu})^{-\lambda}I_{\lambda+n}(m\boldsymbol{\nu})$
Elementary 6 to 10, Bessel 3 & 4	$\exp(-\boldsymbol{\nu}\boldsymbol{a})\exp(-\boldsymbol{\nu}\,\arccos(s))$	$\exp(-m\boldsymbol{\nu}\boldsymbol{a})f(m\boldsymbol{\nu},n)\,(\lambda+n)\,\Gamma(\lambda)\,\Gamma(\lambda+1)\,\frac{\left\lvert\Gamma\left(\frac{n+\iota\,m\boldsymbol{\nu}}{2}\right)\right\rvert^2}{\left\lvert\Gamma\left(\lambda+1+\frac{n+\iota\,m\boldsymbol{\nu}}{2}\right)\right\rvert^2}$
Hypergeometric 1, 3, 5, 7, 9	$\exp(-\nu\boldsymbol{a})\exp(-\nu\,\arccos(s))$	$\exp(-m\nu\boldsymbol{a})f(m\nu,n)\,(\lambda+n)\,\Gamma(\lambda)\,\Gamma(\lambda+1)\,\frac{\left\lvert\Gamma\left(\frac{n+\iota\,m\nu}{2}\right)\right\rvert^2}{\left\lvert\Gamma\left(\lambda+1+\frac{n+\iota\,m\nu}{2}\right)\right\rvert^2}$
Hypergeometric 2, 4, 6, 8, 10	$\exp(-\nu(1+\boldsymbol{a}))\exp(\nu\,s)$	$\exp(-m\nu(1+\boldsymbol{a}))2^\lambda\Gamma(\lambda)(\lambda+n)(m\nu)^{-\lambda}I_{\lambda+n}(m\nu)$

Chen, W., Genton, M. G., and Sun, Y. (2021). Space-time covariance structures and models. *Annual Review of Statistics and Its Application*, 8:191–215.
Chilès, J.-P. and Delfiner, P. (2012). *Geostatistics: Modeling Spatial Uncertainty*. Wiley, New York.
Clarke, J., Alegria, A., and Porcu, E. (2018). Regularity properties and simulations of Gaussian random fields on the sphere cross time. *Electronic Journal of Statistics*, 12:399–426.
Cleanthous, G., Porcu, E., and White, P. (2021). Regularity and approximation of Gaussian random fields evolving temporally over compact two-point homogeneous spaces. *Test*, 30(4):836–860.
Cressie, N. and Huang, H.-C. (1999). Classes of nonseparable, spatio-temporal stationary covariance functions. *Journal of the American Statistical Association*, 94(448):1330–1339.
Curriero, F. C. and Lele, S. (1999). A composite likelihood approach to semivariogram estimation. *Journal of Agricultural, Biological, and Environmental Statistics*, 4(1):9–28.
Emery, X., Alegría, A., and Arroyo, D. (2021). Covariance models and simulation algorithm for stationary vector random fields on spheres crossed with Euclidean spaces. *SIAM Journal on Scientific Computing*, 43(2):A3114–A3134.
Emery, X., Arroyo, D., and Mery, N. (2022). Twenty-two families of multivariate covariance kernels on spheres, with their spectral representations and sufficient validity conditions. *Stochastic Environmental Research and Risk Assessment*, 36:1447–1467.
Emery, X. and Porcu, E. (2019). Simulating isotropic vector-valued Gaussian random fields on the sphere through finite harmonics approximations. *Stochastic Environmental Research and Risk Assessment*, 33(8-9):1659–1667.
Erb, W. and Filbir, F. (2008). Approximation by positive definite functions on compact groups. *Numerical Functional Analysis and Optimization*, 29(9–10):1082–1107.
Genton, M. G. and Kleiber, W. (2015). Cross-covariance functions for multivariate geostatistics. *Statistical Science*, 30(2):147–163.
Gneiting, T. (2002). Stationary covariance functions for space-time data. *Journal of the American Statistical Association*, 97:590–600.
Gneiting, T. (2013). Strictly and non-strictly positive definite functions on spheres. *Bernoulli*, 19(4):1327–1349.
Guella, G. and Menegatto, V. (2016). Strictly positive definite kernels on a product of spheres. *Journal of Mathematical Analysis and Applications*, 435:286–301.
Guella, J. and Menegatto, V. (2019). Positive definite matrix functions on spheres defined by hypergeometric functions. *Integral Transforms and Special Functions*, 30(10):774–789.
Guella, J., Menegatto, V., and Peron, A. (2015). An extension of a theorem of Schoenberg to products of spheres. *Banach Journal of Mathematical Analysis*, 435:286–301.
Guella, J. C., Menegatto, V. A., and Peron, A. P. (2016). An extension of a theorem of Schoenberg to products of spheres. *Banach Journal of Mathematical Analysis*, 10(4):671–685.
Guinness, J. and Fuentes, M. (2016). Isotropic covariance functions on spheres: some properties and modeling considerations. *Journal of Multivariate Analysis*, 143:143–152.
Haaland, B. and Qian, P. Z. (2011). Accurate emulators for large-scale computer experiments. *Annals of Statistics*, 39(6):2974–3002.
Hofmann, T., Scholkopf, B., and Smola, A. (2008). Kernel methods in machine learning. *Annals of Statistics*, 36(3):1171–1220.
Huang, C., Zhang, H., and Robeson, S. (2011). On the validity of commonly used covariance and variogram functions on the sphere. *Mathematical Geosciences*, 43:721–733.
Jeong, J., Jun, M., and Genton, M. G. (2017). Spherical process models for global spatial statistics. *Statistical Science*, 32(4):501–513.
Lang, A. and Schwab, C. (2015). Isotropic Gaussian random fields on the sphere: Regularity, fast simulation and stochastic partial differential equations. *Annals of Applied Probability*, 25(6):3047–3094.
Lantuéjoul, C., Freulon, X., and Renard, D. (2019). Spectral simulation of isotropic Gaussian random fields on a sphere. *Mathematical Geosciences*, 51(8):999–1020.
Mastrantonio, G., Jona Lasinio, G., and Gelfand, A. (2016). Spatio-temporal circular models with non-separable covariance structure. *Test*, 25:331–350.

Mastrantonio, G., Jona Lasinio, G., Pollice, A., Capotorti, G., Teodonio, L., Genova, G., and Blasi, C. (2019). A hierarchical multivariate spatio-temporal model for clustered climate data with annual cycles. *Annals of Applied Statistics*, 13(2):797–823.

Musin, O. R. (2008a). Bounds for codes by semidefinite programming. *Proceedings of the Steklov Institute of Mathematics*, 263(1):134–149.

Musin, O. R. (2008b). Positive definite functions in distance geometry. In *Fifth European Congress of Mathematics*, pages 115–134. European Mathematical Society.

Olver, F. W., Lozier, D. M., Boisvert, R. F., and Clark, C. W. (2010). *NIST Handbook of Mathematical Functions*. Cambridge University Press, Cambridge.

Peron, A., Porcu, E., and Emery, X. (2018). Admissible nested covariance models over spheres cross time. *Stochastic Environmental Research and Risk Assessment*, 32(11):3053–3066.

Porcu, E., Bevilacqua, M., and Genton, M. G. (2016). Spatio-temporal covariance and cross-covariance functions of the great circle distance on a sphere. *Journal of the American Statistical Association*, 111(514):888–898.

Porcu, E., Furrer, R., and Nychka, D. (2021). 30 years of space–time covariance functions. *Wiley Interdisciplinary Reviews: Computational Statistics*, 13(2):e1512.

Porcu, E. and White, P. A. (2022). Random fields on the hypertorus: Covariance modeling and applications. *Environmetrics*, page e2701.

Reams, R. (1999). Hadamard inverses, square roots and products of almost semidefinite matrices. *Linear Algebra and its Applications*, 288:35–43.

Rodrigues, A. and Diggle, P. (2010). A class of convolution based models for spatio-temporal processes with non-separable covariance structure. *Scandinavian Journal of Statistics*, 37(4):553–567.

Schoenberg, I. J. (1942). Positive definite functions on spheres. *Duke Mathematical Journal*, 9(1):96–108.

Shirota, S. and Gelfand, A. (2017). Space and circular time log Gaussian Cox processes with application to crime event data. *Annals of Applied Statistics*, 11(2):481–503.

Stein, M. L. (2005). Space-time covariance functions. *Journal of the American Statistical Association*, 100(469):310–321.

Varin, C. and Vidoni, P. (2005). A note on composite likelihood inference and model selection. *Biometrika*, 92(3):519–528.

White, P. and Porcu, E. (2019). Nonseparable covariance models on circles cross time: A study of Mexico City ozone. *Environmetrics*, page e2558.

Xu, Y. (2018). Positive definite functions on the unit sphere and integrals of Jacobi polynomials. *Proceedings of the American Mathematical Society*, 146(5):2039–2048.

Yaglom, A. M. (1987). *Correlation theory of stationary and related random functions. Vol. I.* Springer Series in Statistics. Springer-Verlag, New York. Basic results.